# Molecular insights into mechanisms of hepatoblastoma pathogenesis

Katja Eloranta

Doctoral Programme in Clinical Research
Doctoral School in Health Sciences
Pediatric Graduate School

Children's Hospital
University of Helsinki
Finland


ACADEMIC DISSERTATION

To be presented, with the permission of the Medical Faculty of the University of Helsinki, for public examination in Biomedicum Helsinki, Lecture Hall 2, Haartmaninkatu 8, Helsinki, on June 10th, 2021, at 12 noon.

Helsinki 2021

**Supervisors**

Professor Markku Heikinheimo, MD, PhD
Children's Hospital
University of Helsinki
Helsinki, Finland

Docent Marjut Pihlajoki, PhD
Children's Hospital
University of Helsinki
Helsinki, Finland

**Reviewers**

Professor Anna-Liisa Levonen, MD, PhD
A.I. Virtanen Institute for Molecular Sciences
University of Eastern Finland
Kuopio, Finland

Professor Risto Kerkelä, MD, PhD
Department of Pharmacology and Toxicology
University of Oulu
Oulu, Finland

**Official opponent**

Docent Olli Lohi, MD, PhD
Department of Pediatrics
Hematology and Oncology Division
Tampere University Hospital
Tampere University
Tampere, Finland

The Faculty of Medicine uses the Urkund system (plagiarism recognition) to examine all doctoral dissertations.

Cover design: Noora Isoaho

ISBN 978-951-51-7312-6 (paperback)
ISBN 978-951-51-7313-3 (PDF)

Unigrafia, Helsinki University Printing House
Helsinki 2021

*To my parents*

# ABSTRACT

Hepatoblastoma (HB) is the most common pediatric liver malignancy with an annual incidence of 1.8 cases per million children. The median age at diagnosis is 1-year-old. Most cases are sporadic, although certain genetic disorders such as Beckwith-Wiedemann syndrome and familial adenomatous polyposis are associated with increased risk of HB.

Developmental pathways, such as WNT/β-catenin and Hedgehog signaling, are often aberrantly activated in HB cells. The overall mutation burden in HB is generally low, but the *CTNNB1* gene encoding β-catenin is altered in over 60 % of cases. HB histology resembles embryonal or fetal liver. Functions carried out in developing liver, like alpha-fetoprotein synthesis and extramedullary hematopoiesis, are also characteristic of HB.

Surgical resection of tumor is a mainstay of HB treatment, generally supported by pre- and post-operative chemotherapy. Platinum-derivatives and doxorubicin form the cornerstone of pharmaceutical HB management, though multiorgan toxicity limits the use of these drugs. The survival rate of HB is over 80 % if tumor is confined to liver but decreases dramatically when there is extrahepatic involvement, so new treatment options are needed.

In this thesis we examined two key factors, GATA4 and neuropilin-2, in the pathobiology of HB. Additionally, we conducted *in vitro* experiments investigating the potential of chloroquine as a novel HB therapy. For these analyses, we used patient tumor samples and multiple HB cell lines cultured in both two- and three-dimensional formats.

Transcription factor GATA4 is crucial for early liver development. We observed that most HB patient samples and cell lines express high levels of GATA4. To investigate its role in oncogenesis, we silenced *GATA4* expression in HUH6 HB cells via small interfering RNA (siRNA) transfection. We performed mRNA microarray hybridization to identify genes affected by *GATA4* knockdown. Genes related to epithelial-mesenchymal transition (EMT) were dysregulated after *GATA4* silencing. Immunofluorescence staining demonstrated increased E-cadherin expression and decreased N-cadherin expression after *GATA4* knockdown, suggesting reversed EMT. We also observed reduced actin polymerization and lower migration rate in *GATA4* silenced cells, implying that GATA4 promotes a more aggressive mesenchymal phenotype in HB cells.

Neuropilins (NRP) are multifunctional receptors involved both in physiological and pathological processes. In cancer cells abundant NRP expression is associated with chemoresistance, increased proliferation, and higher metastasis rate. We noted high *NRP1* and *NRP2* expression in HB patient samples and six HB cell models. Utilizing siRNA transfection, we observed decreased viability and motility in *NRP2* knockdown cells compared to HB cells with intact gene expression. Furthermore, actin

depolymerization increased and cell protrusions decreased after *NRP2* silencing in HB cells suggesting that NRP2 expression promotes malignant behavior in HB.

Chloroquine is a traditional anti-malarial which has demonstrated potential in cancer management both *in vitro* and *in vivo*. We observed a drastic decrease in HB spheroid viability after chloroquine treatment. Moreover, chloroquine triggered increased apoptosis in most of the cell culture models studied. Chloroquine treatment also modified the metabolic profile of HB cells with a remarkable decrease in $NAD^+$ and aspartate concentrations. Death pathway qPCR array demonstrated decreased poly(ADP)-ribose polymerase (*PARP*)1/2 expression after chloroquine treatment, and this was confirmed with protein analysis. Taken together, we demonstrated that chloroquine has anti-tumorigenic potential in HB cell models and its mechanism of action may be linked to altered DNA repair.

In summary, this thesis shed new light on the molecular mechanisms of HB pathogenesis. In the future, these findings may be utilized in development of novel treatment approaches and diagnostics to improve survival and life quality of HB patients.

## Table of contents

# LIST OF ORIGINAL PUBLICATIONS

**This doctoral thesis is based on the following publications:**

**I** Soini, T.*, **Eloranta, K**.*, Pihlajoki, M.*, Kyrönlahti, A., Akinrinade, O., Andersson, N., Lohi, J., Pakarinen, M. P., Wilson, D. B., & Heikinheimo, M. (2018). Transcription factor GATA4 associates with mesenchymal-like gene expression in human hepatoblastoma cells. Tumor Biology, 40(7), 1010428318785498. doi: 10.1177/1010428318785498

II **Eloranta, K.**, Nousiainen, R., Cairo, S., Pakarinen, M. P., Wilson, D. B., Pihlajoki, M., & Heikinheimo, M. Neuropilin-2 is associated with increased cell viability and motility in hepatoblastoma. Submitted.

III **Eloranta, K.**, Cairo, S., Liljeström, E., Soini, T., Kyrönlahti, A., Judde, J. G., Wilson, D. B., Heikinheimo, M., & Pihlajoki, M. (2020). Chloroquine Triggers Cell Death and Inhibits PARPs in Cell Models of Aggressive Hepatoblastoma. Frontiers in Oncology, 10: 1338. doi: 10.3389/fonc.2020.01138

*The authors contributed equally to the study.

The publications are referred to in the text by their roman numerals. In addition, this thesis includes unpublished results.

Publication I has also been used in the thesis of Tea Soini, M.D., PhD, entitled "Transcription factors GATA4 and GATA6 in pediatric liver diseases" (ISBN:978-951-51-4137-8).

# ABBREVIATIONS

| | |
|---|---|
| ABL1 | tyrosine-protein kinase ABL1 |
| ADD3 | adducin 3 |
| AFP | alpha-fetoprotein |
| AHNAK | AHNAK nucleoprotein |
| ALDH2 | aldehyde dehydrogenase 2 family member |
| APCS | serum amyloid P-component |
| APOC4 | apolipoprotein C-IV |
| AQP9 | aquaporin 9 |
| BECN1 | beclin-1 |
| BMP | bone morphogenetic protein |
| BUB1 | mitotic checkpoint serine/threonine-protein kinase |
| C/EBP | CCAAT-enhancer binding protein |
| C1S | complement component 1S |
| CD40 | tumor necrosis factor receptor superfamily member 5 |
| CD40LG | CD40 ligand |
| CDH1 | E-cadherin |
| CDH2 | N-cadherin |
| COL4A1 | collagen alpha-1(IV) chain |
| CQ | chloroquine |
| CTNNB1 | beta-catenin |
| CTSS | cathepsin S |
| CYP2E1 | cytochrome P450 2E1 |
| DKK | dickkopf-related protein |
| DLGAP5 | disks large-associated protein 5 |
| DOCK8 | dedicator of cytokinesis protein 8 |
| DPYSL4 | dihydropyrimidinase-related protein 4 |
| DUSP9 | dual specificity protein phosphatase 9 |
| E2F5 | transcription factor E2F5 |
| EMT | epithelial-mesenchymal transition |
| ESR1 | estrogen receptor |
| FGF | fibroblast growth factor |
| FOXA | forkhead box protein A |
| FOXI1 | forkhead box I1 |
| GAL | galectin |
| GATA | GATA binding protein |
| GHR | growth hormone receptor |
| HB | hepatoblastoma |
| HCC | hepatocellular carcinoma |
| HGF | hepatocyte growth factor |
| HHEX | haematopoietically-expressed homeobox factor |
| HNF | hepatocyte nuclear factor |
| HPD | 4-hydroxyphenylpyruvate dioxygenase |
| HSC | hepatic stellate cell |
| IFNG | interferon gamma |

| | |
|---|---|
| IGF | insulin-like growth factor |
| IGFBP1 | insulin-like growth factor binding protein 1 |
| IGSF1 | immunoglobulin superfamily member 1 |
| LSEC | liver sinusoidal endothelial cell |
| MMP1 | matrix metalloproteinase 1 |
| MSF | migration stimulatory factor |
| NAD | nicotinamide adenine dinucleotide |
| NLE1 | notchless protein homolog 1 |
| NRP | neuropilin |
| OC | onecut |
| PARP | poly(ADP)-ribose polymerase |
| PDGF | platelet-derived growth factor |
| PDX | patient-derived xenograft |
| PH | primary hepatocyte |
| PIGF | placental growth factor |
| RHOB | Ras homolog gene family, member B |
| RHOU | Ras homolog gene family, member U |
| RPL10A | ribosomal Protein L10a |
| SCUD | small cell undifferentiated |
| siRNA | small interfering RNA |
| SOX | SRY-box transcription factor |
| SQSTM1 | sequestosome 1 |
| SRC | SRC proto-oncogene, non-receptor tyrosine kinase |
| SYTL2 | synoptotagmin-like 2 |
| Tbx | T-box transcription factor |
| TGFβ | transforming growth factor beta |
| TNF | tumor necrosis factor |
| TP53 | tumor protein P53 |
| TXNL4B | thioredoxin Like 4B |
| VEGF | vascular endothelial growth factor |
| YAP1 | Yes associated protein 1 |

# REVIEW OF THE LITERATURE

## 1 LIVER

### **1.1** Development

The post-gastrulation embryo is composed of three germ layers: ectoderm, mesoderm, and endoderm. Liver develops from endoderm, the innermost germ layer. The process of hepatogenesis can be divided into three major stages: hepatic specification, liver bud formation and growth, and epithelial differentiation (**Figure 1**) [reviewed in (1)].

Hepatic specification entails establishment of hepatic competence in the ventral foregut endoderm resulting in the appearance of hepatoblasts. Forkhead box protein A (FOXA) (2) and GATA transcription factors (GATA4/6) (3) modify chromatin structure to unmask hepatic gene regions enabling their subsequent activation. During hepatoblast specification, foregut endoderm closely interacts with septum transversum mesenchyme and cardiac mesoderm. Animal studies have shown that bone morphogenetic proteins (BMPs) and fibroblast growth factors (FGFs) play important roles in inducing gene expression pattern leading to the rise of hepatoblasts (4,5).

In the next phase of organogenesis, hepatoblasts invade septum transversum mesenchyme forming a liver bud. Thereafter, hepatoblasts proliferate rapidly and the nascent liver expands under the influence of signals from septum transversum mesenchymal cells and neighboring endothelial cells (reviewed in 1). Several transcription factors have been recognized to take a part to this process, including GATA4/6, hepatocyte nuclear factor 6 (HNF6), onecut 2 (OC2), prospero-related homeobox 1 (Prox1), haematopoietically-expressed homeobox factor (HHEX), and T-box transcription factor 3 (Tbx3) [reviewed in (6)].

Shortly after liver bud formation, bipotential hepatoblasts start to differentiate into hepatocytes and cholangiocytes. This process commences approximately at gestation week 9 in humans and continues until the beginning of the last trimester (7,8). The mechanisms regulating liver epithelial differentiation are not fully understood, but HNF1α, HNF4α, and CCAAT/enhancer binding protein-α (9) have have significant roles in hepatocyte lineage specification, whereas HNF1α, SRY-Box transcription factor (SOX)4/9, and HNF6 are associated with cholangiocyte fate determination (10,11).

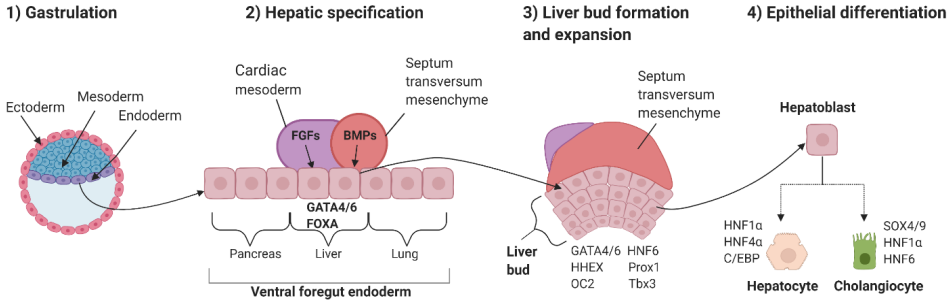


**Figure 1. Simplified view of the liver development from gastrulation to epithelial differentiation.** *During the early embryogenesis, three germ layers are formed (1). Cells derived from the endoderm achieve hepatic competence leading to the rise of hepatoblasts (2). Hepatoblasts migrate into the septum transversum mesenchyme and proliferate rapidly, which is orchestrated by various signals (3). Hepatoblasts differentiate into cholangiocytes and hepatocytes under the influence of certain HNFs, SOX4/9, and C/EBP (4). Figure was created with BioRender.com.*

## 1.2 Gross anatomy

The liver resides in the upper-right quadrant of the abdominal cavity, inferior to the diaphragm and superior to the stomach, intestines, and right kidney. The liver is the second largest organ in the human body weighting approximately 1400-1800 g in adults (12) and 150 g in the newborns (13). The organ is divided into two lobes (right and left) separated by falciform ligament, which joins the liver to the anterior abdominal wall. Functionally, the liver can be further divided into eight segments (**Figure 2**) based on blood supply and bile drainage (14). The liver receives blood from two sources: oxygenated blood comes from the hepatic artery (20 %) and portal vein (80 %) brings blood from the intestines. Outflow from the liver is directed to three major hepatic veins terminating in the inferior vena cava.

Biliary anatomy is composed of intrahepatic and extrahepatic parts (15). Intrahepatic bile canaliculi drain bile to the hepatic ducts which unite to form the common hepatic duct. Outside the liver, the common hepatic duct joins with the cystic duct originating from the gallbladder. These two ducts form a common cystic duct draining bile into the duodenum.

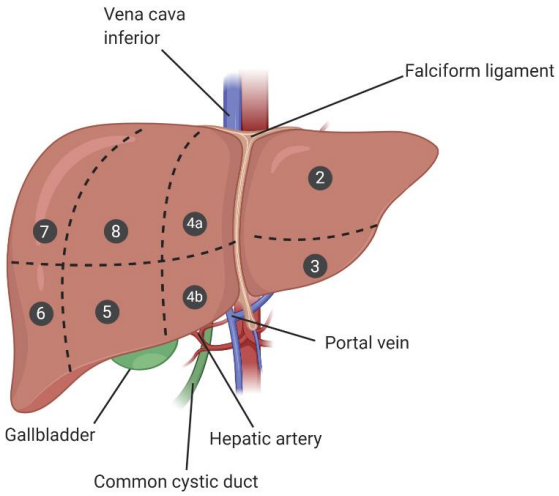


**Figure 2. Segmental anatomy of the liver.** *Segment 1 is located on the posterior side of the liver (not shown). Figure was created with BioRender.com.*

### 1.3 Function

Physiologically, the liver has an essential role in coordinating anabolic and catabolic reactions, homeostasis, and excretion of waste products in the human body [reviewed in (16)]. It orchestrates carbohydrate, amino acid, and lipid metabolism and participates in drug metabolism, detoxification, and secretion of xenobiotic substances. In addition to secreting numerous proteins such as coagulation factors, albumin, and insulin-like growth factor 1, the liver aids digestion through bile production. In collaboration with other organs, the liver controls body temperature and assists in the maintenance of blood volume. Certain minerals, such as iron and copper, are stored in the liver together with fat-soluble vitamins. During fetal development, the liver is also the main hematopoietic organ.

The functional unit of the liver is a hexagonal structure called a lobule (**Figure 3A**), composed of hepatocyte cords covered with endothelial cells constituting sinusoids. Each hexagon corner contains a branch of the hepatic artery, portal vein, and bile duct, together forming a structure named the portal triad. Branches of the hepatic artery and portal vein drain blood to sinusoids; outflow from sinusoids collects in the central vein of each lobule and then into the hepatic veins. As a consequence of this structural organization, blood perfusion and metabolism are dissimilar in hepatocytes nearest to the portal triad versus those next to the central vein (17). The acinus is the smallest functional structure in the liver dividing hepatocytes in three zones depending on their position within the lobule.

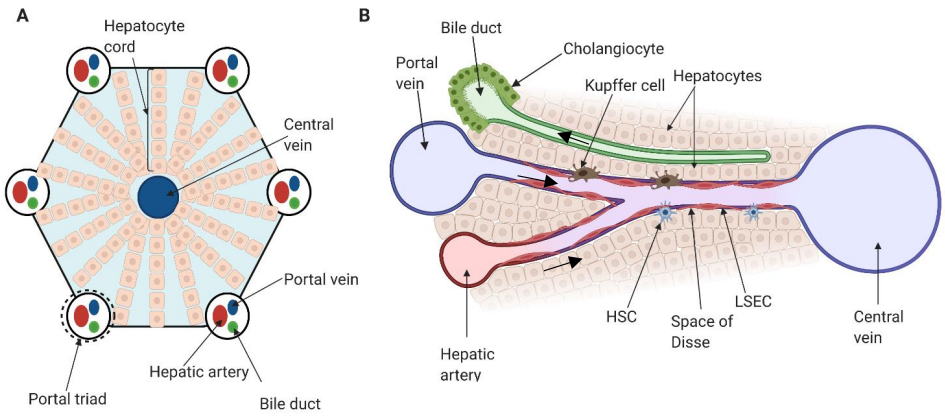


**Figure 3. Structure of the liver lobule and main cell types.** *A lobule is composed of hepatocyte cords lined with LSECs, a portal triad in each corner, and central vein in the middle (A). Hepatocytes, cholangiocytes, Kupffer cells, LSECs, and HSCs make up the vast majority of cells residing in the liver (B). Arrows indicate flow direction inside the structures (B). HSC=hepatic stellate cell. LSEC=liver sinusoidal endothelial cell. Figure was created with BioRender.com.*

### 1.4 Cellular anatomy and physiology

Liver parenchyma is composed of polygonal-shaped hepatocytes comprising approximately 80 % of all the cells in the organ. The basal surface of hepatocytes faces the perisinusoidal space (Space of Disse) (**Figure 3B**) and associated liver sinusoidal endothelial cells (LSECs). The apico-lateral surface interacts with neighboring hepatocytes and bile ducts. This polarization has physiological significance; the apical surface mainly secretes bile, while the basal side is important for secretion and uptake of nutrients, hormones, and proteins to/from circulation. Key physiological processes involving hepatocytes are listed in **Table 1**.

The liver has great regeneration potential, and in adult liver new hepatocytes are thought to arise from oval cells. These cells are bipotential liver progenitor cells which are able to differentiate into hepatocytes and cholangiocytes as response to injury [reviewed in (18)].

The main non-parenchymal cell types in liver include cholangiocytes, Kupffer cells and other macrophages, LSECs, pit cells, and hepatic stellate cells (**Figure 3B**). Small populations of lymphocytes also reside in liver.

Cholangiocytes are cuboidal-shaped epithelial cells forming bile ducts. They regulate bile composition and transport. LSECs are fenestrated cells forming sinusoids. Fenestrae and gaps between LSECs allow easy exchange of substances between hepatocytes and the blood stream. Kupffer cells responsible for front-line innate immune reactions constitute the major macrophage population in liver. Quiescent hepatic stellate cells

store lipids and vitamin A, and in response to inflammation these cells transform to myofibroblasts.

Recent single cell RNA sequencing studies have shown that liver cell types can be further divided into discrete subpopulations; over 20 distinct cell types have been identified in the adult liver (19,20).

**Table 1. Liver cell types and their role in the physiological processes.** *Table modified from* (21).

| Cell type | Location in liver | Physiology |
|---|---|---|
| Hepatocyte | Parenchyma | glucose/glycogen metabolism, cholesterol metabolism, bile secretion, xenobiotic metabolism, urea metabolism, blood clotting, acute phase response, protein secretion |
| Cholangiocyte | Ductal epithelium | bile duct structure, controls bile transport and flow rate, secrete water and bicarbonate |
| Liver sinusoidal endothelial cell | Sinusoids | facilitate blood microcirculation by forming sinusoids, allow transfer of proteins and other molecules between blood and hepatocytes, cytokine secretion, blood clotting, immune responses |
| Endothelial cell | Vasculature | form blood vessels, contribute to hepatic zonation |
| Kupffer cell | Sinusoids | phagocytosis of foreign material, secretion of cytokines and proteases, innate immunity |
| Hepatic stellate cells | Perisinusoidal | lipid, vitamin A, and retinoid storage, contribute to extracellular matrix maintenance and response to injury, secrete cytokines |
| Pit cell | Sinusoids | natural killer cell activity |

# 2 HEPATOBLASTOMA

## 2.1 Epidemiology and etiology

Hepatic neoplasms are rare in childhood, and malignant liver tumors account approximately 65 % of the cases [reviewed in (22)]. Hepatoblastoma (HB) is the most common liver cancer type among the infants and young children with an annual incidence of 1.9 patients per million (23). Between 1987 and 2016, the median HB incidence in Finland was 1.1 cases per million (24). Most cases of HB present before 5 years of age, and the median age at diagnosis is 1 year (23,25). Other primary liver malignancies in pediatric population include hepatocellular carcinoma (HCC), which typically occurs later in childhood, and sarcomas [reviewed in (26)]. Tumors having features of both HB and HCC exist, and these are classified as transitional liver cell tumors (27).

In most cases the etiology of HB is obscure, although histology and molecular landscape allude to a developmental origin [reviewed in (28)]. Male predominance has been observed in several studies (29,30). Certain genetic syndromes are associated with higher risk for HB, including Beckwith-Wiedemann syndrome, Sotos syndrome, familial adenomatous polyposis, and trisomy 18 (31–36).

Low birth weight is a clear risk factor for HB (37–40). Exposure to environmental factors during the perinatal period, such as pre-eclampsia, maternal tobacco consumption, and infertility treatments have been investigated as potential HB risk factors, but conclusions have been inconsistent (37,41,42).

## 2.2 Diagnosis

A palpable mass or abdominal swelling are the typical presenting signs of HB. Patients may also exhibit nausea, vomiting, weight loss, growth retardation, abdominal pain, jaundice, or lethargy.

Serum alpha-fetoprotein (AFP) is commonly elevated in HBs and is a key tumor marker for diagnosis and surveillance. Some aggressive HBs, however, are associated low serum AFP levels (43). Other serum biomarkers proposed for HB diagnostics include microRNA-21, glypican-3 (GPC3), hepatocyte derived lipocalin-2, and delta-like 1, but none of these is currently in widespread clinical use (44–47).

Radiological examination including ultrasonography, computed tomography, and magnetic resonance imaging are employed to evaluate tumor size and delineate affected areas (48). Additionally, diagnostic biopsy is essential to confirm the diagnosis of HB.

### 2.3 Histology

HB histology is heterogenous. This heterogeneity is evident between tumors and even in different regions of the same tumor. Tumor cells may exhibit various differentiation stages, and tumors may include teratoid components. Generally HBs can be classified into two groups: pure epithelial (56 %) and mixed epithelial and mesenchymal tumors (44 %) (48,49).

Based on cell differentiation stage and growth pattern, pure epithelial HBs are further divided into five subtypes. Tumor components may resemble fetal or embryonal hepatoblasts, demonstrate loss of cell architecture characteristic for small-cell undifferentiated (SCUD) form, have macrotrabecular organization, or express cholangiocyte markers typical for cholangioblastic HB (50,51). Hepatoblasts produce AFP during normal liver development and this feature is present in a majority of HBs (52,53). Extramedullary hematopoiesis is commonly observed in fetal areas of HBs (54). SCUD histology rising from poorly differentiated stem cells is associated with low AFP expression and serum concentration (43). Other markers suggested for histological evaluation of HBs include GPC3, β-catenin (CTNNB1), and integrase interactor 1 (INI1) [reviewed in (55)].

In addition to epithelial components, HBs with mixed histology contain stromal derivatives, such as osteoid, cartilage, or spindle cells, with or without teratoids (54).

### 2.4 Molecular biology

Whole chromosome aneuploidies are frequent in HB. Genomic gains most often affect chromosomes 2, 8, and 20, whereas genomic losses are typically observed in chromosome 18 [reviewed in (56)]. Structural alterations are less common, though an unbalanced translocation involving long arm of chromosome 1 has been reported in several studies (57,58). Gains of chromosomes 8q and 2p are linked to aggressive form of HB (59).

HBs harbor a relatively low mutation burden, which is typical of other pediatric cancers. Deregulated pathways are associated with developmental signaling. WNT/β-catenin signaling is often aberrantly activated in cancer cells and promotes tumor progression by regulating proliferation, motility, and stem cell renewal [reviewed in (60)]. In HB, mutations in *CTNNB1* gene encoding β-catenin are observed approximately in 65 % of cases (61,62). Mutations in other genes (*AXIN*2, *DKK1*, *DKK3*) related to WNT/β-catenin pathway are also common (63,64). Additionally, upregulation of the WNT target gene *MYC* and HGF/c-MET mediated activation of β-catenin have been demonstrated in HBs (59,65,66).

Other developmental pathways implicated in HB pathogenesis include Hedgehog, IGF, and Hippo signaling. The Hedgehog pathway is activated during liver organogenesis, regeneration, and malignant transformation. The Hedgehog ligands GLI1 and PTCH1

are frequently overexpresed in HBs (67). Abnormal IGF-axis activity, including both altered expression of ligands and receptors, was demonstrated in the study by Gray et al (68). Hippo signaling mediator YAP1 has been observed to be overexpressed in large set of HBs, and enforced upregulation of YAP1 in mouse model led to rapid HB formation (69).

There is increasing evidence that certain epigenetic and genetic signatures are associated with HB pathogenesis and prognosis. Cairo et al. identified a signature of 16-genes (**Table 2**) that can be utilized in HB risk assessment (59,70). Two distinct epigenomic subtypes of HB have been demonstrated recently (71).

**Table 2. 16-gene signature associated with poor prognosis in HB** (70)**.**

| Gene symbol | Upregulated ↑ / Downregulated ↓ |
|---|---|
| *BUB1* | ↑ |
| *CYP2E1* | ↓ |
| *C1S* | ↓ |
| *GHR* | ↓ |
| *ALDH2* | ↓ |
| *AFP* | ↑ |
| *DUSP9* | ↑ |
| *IGSF1* | ↑ |
| *APCS* | ↓ |
| *APOC4* | ↓ |
| *HPD* | ↓ |
| *RPL10A* | ↑ |
| *DLGAP5* | ↑ |
| *NLE1* | ↑ |
| *AQP9* | ↓ |
| *E2F5* | ↑ |

## 2.5 Risk stratification and prognosis

Radiological pre-treatment extent of disease (PRETEXT) staging is used to assess tumor distribution before treatment initiation. Based on affected liver segments, tumors are staged PRETEXT I-IV (**Figure 4**) (72). PRETEXT stages are supplemented with annotation factors describing involvement of hepatic vasculature (V, P), extrahepatic growth (E), multifocal nodes (F), tumor rupture at diagnosis (R), or metastasis (M). According to the Children's Hepatic tumors International Collaboration coalition, HBs grouped in PRETEXT III or IV diagnosed in older children (≥3 years) or metastasis or low AFP concentration (≤100 ng/ml) with any PRETEXT stage are categorized as high risk tumors (73). If any VPEFR annotations are involved, tumors belong to intermediate or high-risk group depending on patient age. Young age correlates with lower risk in all PRETEXT classes. Five-year event-free survival is demonstrated to be over 80 % in all

PRETEXT groups if there is no metastasis or VPEFR involved, patient is younger than 3-year old at diagnosis, and AFP > 1000 ng/ml. Event-free survival decreases drastically when metastasis is present, being less than 50 % in five-year period.

Tumor histology also has been associated with prognosis: pure fetal HBs are linked to better overall survival and in some cases these tumors can be resected without chemotherapy (74). Less differentiated and especially SCUD histology have been suggested to be unfavorable predictors of event- and over-all survival (75).

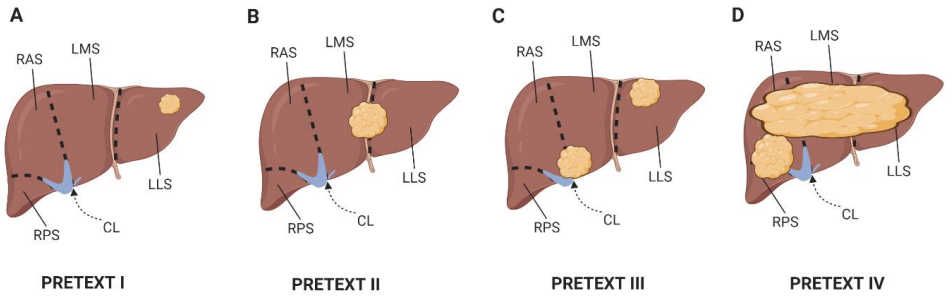


**Figure 4. Radiological PRETEXT staging describes which liver sections are affected by tumor.** *PRETEXT I includes situations when tumor is only in one section (RPS or LLS) and there are three tumor-free adjoining sectors (A). Tumors affecting on two sections or CL, RAS, or LMS alone are staged PRETEXT II (B). PRETEXT III tumors involve three sectors and there are no tumor-free adjoining sectors (C). When all the sectors are affected (with or without CL), tumors are staged PRETEXT IV (D). RPS=right posterior section. RAS=right anterior section. LMS=left medial section. LLS=left lateral section. CL=caudal lobe. Figure was created with BioRender.com*

## 2.6 Treatment

Complete resection of tumor is a mainstay of HB treatment and is supported by pre- and post-operative chemotherapy. Cisplatin monotherapy is recommended for standard risk patients (76). Patients with more advanced disease are treated with "superPLADO" (cisplatin alternating with carboplatin and doxorubicin) or cisplatin/doxorubicin therapy according to SIOPEL (Childhood Liver Tumors Strategy Group) protocols (77,78). Additionally, there are ongoing clinical trials assessing the efficacy of vincristine, etoposide, irinotecan, 5-fluorouracil, gemcitabine, oxaliplatin, and sorafenib alone or combined with current treatments (clinicaltrials.gov study ID: NCT03017326). Pre-operative chemotherapy aims to shrink the tumor thereby enabling surgical resection. If the tumor remains unresectable, liver transplantation is performed if limiting risk factors (extrahepatic disease) are not present. Overview of HB management is presented in **Figure 5**.

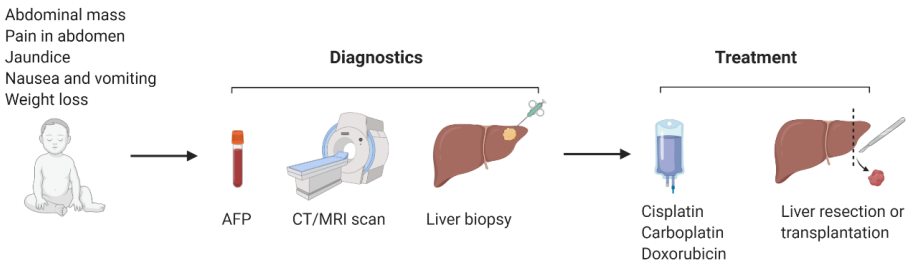


**Figure 5. Schematic view of the HB management.** *Abnormal function and mass in the abdominal area rises a suspicion of HB which is confirmed with laboratory tests (including serum AFP), CT or MRI scan, and histological analysis of tissue biopsy sample (left and middle panel). Surgical treatment combined with chemotherapy forms the cornerstone of HB treatment (right panel). Figure was created with BioRender.com*

# 3 NEUROPILINS

## 3.1 Structure and function

Neuropilins (NRPs) are single-passing type I transmembrane glycoproteins acting typically as co-receptors enforcing the signal transduction (79). NRP family is composed of two members, NRP1 and NRP2, sharing approximately 45 % of sequence homology at amino acid level (**Figure 6**) [reviewed in (80)]. In humans, *NRP1* gene is located in the short arm of chromosome 10 (10p11) and *NRP2* gene is mapped to the long arm of chromosome 2 (2q34) (81). Common structure of NRPs contains seven domains: two complement (CUB) domains (a1 and a2), two coagulation factor (FV/FVIII) domains (b1 and b2), MAM domain (c), transmembrane domain (tm), and cytoplasmic domain (cyto) (82) (**Figure 6**). In addition to membrane-bound NRPs, alternative splicing results also in truncated soluble NRP isoforms lacking MAM, transmembrane and, cytoplasmic regions (83–85).

NRPs have role in multiple physiological and pathological processes due to their versatile co-receptor and ligand assortment. They were originally documented as regulators of neural and vascular development interacting with plexins and vascular endothelial growth factor receptors (VEGFR). NRP2 has also a crucial role in formation of small lymphatic vessels (86). Transgenic mouse model deficient both for NRP1 and NRP2 (*NRP1*$^{-/-}$ and *NRP2*$^{-/-}$) demonstrates severely abnormal vascular phenotype and embryonic lethality is observed before mid-gestation (E8.5) (87). In addition to neural, vascular, and lymphatic systems, postnatal NRP expression has been discovered in various organs including pancreas (pancreatic islet neogenesis), lung (homeostasis of alveolar epithelium), liver (activation of HSCs during the liver regeneration), and thymus (activation of T cells) (88–91). Ligands involved in these processes encompass platelet derived growth factor (PDGF), VEGFs, and semaphorins (SEMA).

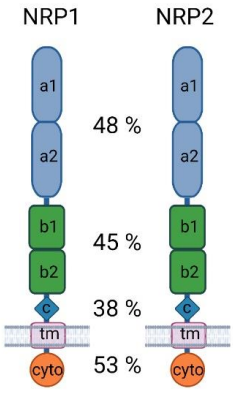


**Figure 6. Structure of NRPs.** *NRPs are composed of seven domains including two CUB domains (a1-a2), two FV/FVIII domains (b1-b2), MAM domain (c), transmembrane domain (tm), and cytoplasmic domain (cyto). Percentages describe the sequence homology in each structural region.*

### 3.2 NRP expression and role in cancer

Abundant NRP1 and/or NRP2 expression has been detected in various solid tumors including pancreatic adenocarcinoma, non-small cell lung cancer, ovarian carcinoma, colon cancer, glioma, neuroblastoma, and HCC (92–99). Mechanistically, NRPs are co-operating with multiple cancer-related signaling pathways (**Figure 7**) encompassing VEGFRs, PDGFR, hepatocyte growth factor (HGF)/c-MET, TGFβR, and integrins [reviewed in (100)].

NRPs are involved in several pro-tumorigenic processes such as proliferation, epithelial-mesenchymal transition (EMT), vascular remodeling, metastasis formation, and chemoresistance [reviewed in (101)]. Additionally, animal studies have shown that blocking NRP function reduces cancer growth and metastasis in tumor models including HCC, glioma, and colorectal carcinoma (102–104). Investigations have demonstrated that NRPs can be utilized also as delivery target for conventional agents such as cisplatin and doxorubicin aiming to increase the treatment specificity and efficacy (105,106).

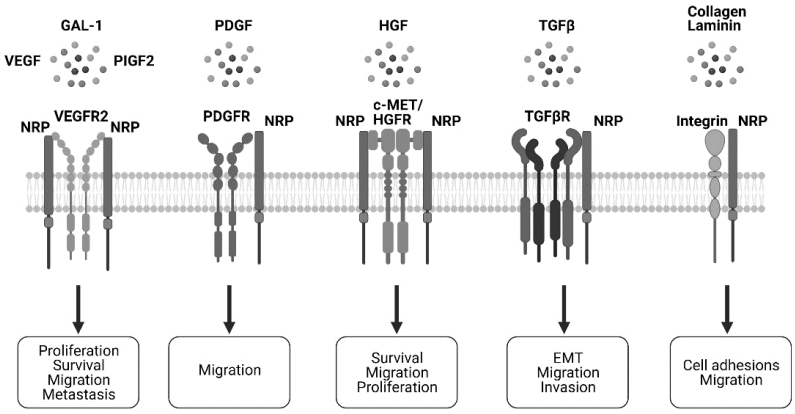


**Figure 7. Overview of the NRP signaling in tumor cells.** *NRPs are typically acting as enhancing co-receptors for multiple cancer related players such as VEGFR2, PDGFR, c-MET/HGFR, TGFβR, and integrins. Figure was created with BioRender.com.*

# 4 INNOVATIVE APPROACHES IN CANCER TREATMENT

## 4.1 Drug re-purposing

Drug re-purposing is a strategy to overcome the slow pace and high cost of discovering new treatment compounds by evaluating drugs already accepted for some other indication for novel purposes [reviewed in (107)]. As the safety is already evaluated during the original market approval process, re-purposed drugs can proceed to phase 2 clinical trials faster than new compounds. Typically "old" drugs are also more cost-effective than novel treatments, which is beneficial from both patient and society point of view.

In oncology, drugs evaluated for cancer treatment represent multiple categories such as non-steroid anti-inflammatory, anti-fungal, vasodilating, antimalarial, and antidepressant agents [reviewed in (108)]. One of widely studied drugs is chloroquine (CQ) which is a classical anti-malarial drug. It has demonstrated anti-tumorigenic actions in various solid cancer types including HCC, pancreatic adenocarcinoma, colon cancer, and glioblastome multiforme (109–112). Furthermore, conventional chemotherapy combined with CQ has shown increased anti-tumor efficacy in several cancer cell models, and this approach has been tested also in clinical use for glioblastoma multiforme (113–115).

## 4.2 Targeted therapies

Conventional cancer therapy is based on cytotoxic chemotherapeutic agents, such as platinum-derivatives and doxorubicin which are utilized in HB management. The major problem in this approach is a multiorgan toxicity as the cellular targets are also widely present in healthy cells (116–118).

Gene and protein expression in cancer cells and their surroundings is remarkably different compared to normal cells. By identifying these molecular alterations, therapeutic modalities targeting tumor specific features have been discovered. Targeted therapies have potential to be less toxic for healthy cells than traditonal cytotoxic agents as their effect is limited mainly to the tumor and its microenvironment [reviewed in (119)]. Additionally, conventional cytotoxic drugs may be conjugated with tumor-targeted molecule which has the potential to increase specificity. An overview of the approaches for molecular targeting in cancer are shown in **Figure 8**.

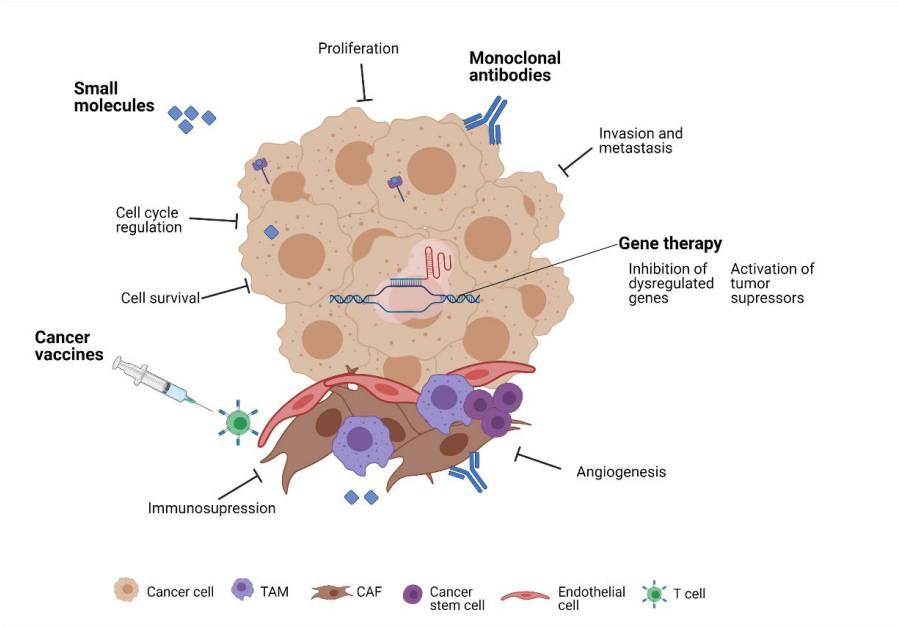


***Figure 8. Molecular targeting in cancer cells and tumor microenvironment.*** *Targeted therapies can be focused on either directly to the tumor cells or cells residing in the microenvironment. TAM=tumor associated macrophage. CAF=cancer associated fibroblast. Figure was created with BioRender.com.*

### 4.3 Monoclonal antibodies

Monoclonal antibodies commonly target proteins located on the extracellular side of the cell membrane. These targets include membrane-bound receptors, soluble receptors, and circulating signaling molecules. Mechanism of action can be based on direct disruption of tumor cell function (e.g., inhibition of survival signals) or it can be executed undirectly through immune response activation (e.g., antibody dependent cellular cytotoxicity) [reviewed in (120)].

Overexpression of epithelial cell adhesion molecule (EpCAM) has been observed in HBs (121), and Armeanu-Ebinger and colleagues suggested that targeting EpCAM with monoclonal antibody may be beneficial in HB treatment (122).

### 4.4 Small molecules

Small molecule (<900 Da) drugs are typically able to penetrate into cells which allows targeting to intracellular proteins. Common targets include proteins involving cell cycle

coordination (e.g., CDK inhibitors), dysfunctional apotosis (e.g. BAX agonists), and aberrant DNA-damage repair response (e.g., PARP inhibitors) (123–125).

In HB, the PLK1 inhibitor volasertib and proteasome inhibitor bortezomib have been shown to have efficacy in pre-clinical studies (126,127). Monotherapy with multikinase inhibitor sorafenib has been tested for refractory HB with encouraging results in case study Shanmugam et. al (128).

### 4.5 Gene therapy and cancer vaccines

Gene therapy aims to modify, inhibit, or activate gene expression to the direction which is harmful for the cancer cells. This can be carried out utilizing multiple methods including oncolytic viruses, RNA interference, CRISPR-Cas9 mediated gene editing, and oligonucleotide therapeutics [reviewed in (129)]. RNA interference therapy employs small RNA molecules to regulate gene expression and CRISPR-Cas9 is able to edit gene structure specifically enabling replacement of the unfunctional gene (130,131).

Lu et al. published recently results from first human trial employing CRISPR technology in cancer treatment. They observed a relatively low rate of off-target effects increasing the potential of CRISPR as a future cancer therapeutic modality (132). MicroRNA therapies have been tested in pre-clinical studies for HB treatment including targeting to microRNA-4510 and microRNA-624-5p (133,134).

Cancer vaccines aim to stimulate T cell mediated immune response against tumor cells. Briefly, proteins from tumor cells are identified and these are presented to the body as antigens (135).

# AIMS OF THE STUDY

This doctoral thesis focuses on molecular mechanisms in the HB pathobiology.

The specific aims of studies presented in this thesis are:

1. To elucidate the role of transcription factor GATA4 in HB pathogenesis and identify the genes associated with GATA4.

2. To assess the expression pattern of neuropilin-2 in HB and investigate its potential as a treatment target.

3. To evaluate the efficacy of chloroquine in HB cells and enlighten its molecular mechanisms of action in cancer.

# MATERIAL AND METHODS

## 1 Patient samples and clinical data (I, II)

HB patients included in this study were treated at Children's Hospital in Helsinki University Hospital between January 1st, 1990 and December 31st, 2017. Samples were originally collected during the diagnostic procedures or surgical treatment. Normal liver control samples were obtained from organ donors. Clinical data was acquired from patient medical record system of Helsinki University Hospital. This study was approved by board of Helsinki University Hospital Ethical Committee (98/13/03/03/2013, HUS/3319/2018) and Finnish National Authority of Medicolegal Affairs and Health (THL/1239/5.05.01/2015).

## 2 Cell cultures

### 2.1 Cell lines (I, II, III)

Eight human HB cell lines were utilized in studies included in this thesis. Characteristics of each cell line are described in **Table 3**. Immortalized HUH6 cell line was purchased from Japanese Collection of Research Bioresources Cell Bank (Osaka, Japan) and HepG2 was a kind gift from Professor Timo Otonkoski (University of Helsinki, Finland). Cell lines established from patient-derived xenografts (PDXs; HB-243, HB-279, HB-282, HB-284, HB-295, HB-303) were obtained through collaboration with XenTech (Evry, France). HUH6 and HepG2 cells were maintained in Dulbecco's Modified Eagle's Medium (DMEM)-glutaMAX supplemented with 10 % fetal bovine serum (FBS), 100 U/mL penicillin, and 100 µg/mL streptomycin sulfate (all from Gibco, Waltham, MA, USA). Cell lines established from PDX models were maintained in Advanced DMEM:F12 supplemented with 8 % FBS, 2 mM glutaMAX, 100 U/mL penicillin, and 100 µg/mL streptomycin sulfate, and 20 µM rock kinase inhibitor Y-27632 (S1049; SelleckChem, Houston, TX, USA). All the cell lines were routinely tested for mycoplasma contamination with PCR-based method (PromoCell, Heidelberg, Germany).

**Table 3. Characteristics of the cell lines.**

| Cell line | Age at sampling | Sex | Histology | Origin | Reference | Article |
|---|---|---|---|---|---|---|
| HUH6 | 12 months | male | mixed, predominantly embryonal | primary tumor | (136) | I, II, III |
| HepG2 | 15 years | male | epithelial | primary tumor | (137) | I |
| HB-243 | 52 months | male | embryonal | extrahepatic residual | (126) | II, III |
| HB-279 | 79 months | male | embryonal and macrotrabecular | primary tumor | (126) | II, III |
| HB-282 | 12 months | male | embryonal | primary tumor | (126) | II, III |
| HB-284 | 83 months | male | embryonal | peritoneal metastasis | (126) | II, III |
| HB-295 | 26 months | female | fetal | primary tumor | (126) | II, III |
| HB-303 | 69 months | female | fetal | primary tumor | (138) | II, III |

### 2.2 Primary hepatocytes (I, II)

Cryopreserved primary hepatocytes from donors (51-year old Caucasian male and 4-year old Caucasian male) with non-liver related causes of death were purchased from commercial provider (Lonza, Basel, Switzerland). Cells were cultured on collagen I -coated plates as monolayers and maintained in HBM™ Basal Medium supplemented with transferrin, ascorbic acid, epidermal growth factor, insulin, hydrocortisone, fatty-acid free bovine serum albumin, 30 mg/ml gentamicin and 15 μg/ml amphotericin (all from Lonza).

### 2.3 Spheroid cultures (III)

Cells were seeded (3000 cells/well) into CellCarrier ultra-low attachment surface 96-well plates (PerkinElmer, Waltham, MA, USA). Spheroids were kept undisturbed for 72 h to establish the three-dimensional (3D) structure. After the initiation period, imaging and treatments were conducted.

### 3 Manipulation of gene expression (I, II)

Prior disturbing the gene expression of *GATA4* or *NRP2*, the cells were seeded at density to reach 70-80 % confluency at the time of transfection.

### 3.1 Small interfering RNA transfections (I, II)

Small interfering RNA (siRNA) transfections were used to downregulate expression of selected genes in HB cell cultures. HUH6 (I, II) and HepG2 (I) cells were treated with ON-target Plus SMARTpool siRNAs (Dharmacon, Cambridge, UK) at a final concentration of 100 nM. RNAiMAX lipofectamine reagent (Thermo Fisher Scientific, Waltham, MA, USA) diluted in OptiMEM medium (Gibco) was used to deliver siRNAs into the cells. Non-targeting (NT) siRNAs were used as a control treatment.

### 3.2 Plasmid transfections (I)

Primary hepatocytes were transfected with pMT2-GATA4 (139) or pMT2 control plasmid to enforce overexpression of *GATA4*. Plasmids were delivered into the cells utilizing jetPEI™ Hepatocyte DNA transfection reagent diluted in OptiMEM medium (Gibco).

## 5 RNA expression analysis

### 4.1 RNA extraction and real-time quantitative PCR (I, II)

RNA was extracted utilizing NucleoSpin RNA/Protein kit (Macherey-Nagel, Düren, Germany) and reverse transcription was carried out with Reverse transcriptase core kit (Eurogentec, Seraing, Belgium). Mesa Green qPCR MasterMix Plus SYBR assay (Eurogentec) was employed to carry out real-time quantitative PCR (RT-qPCR). Geometric mean of *PPIG* and *GAPDH* expression was used as reference. Primer sequences are given in **Table 4**.

**Table 4. RT-qPCR primer sequences.**

| Gene symbol | Oligonucleotide sequence (5' → 3') | Reference |
|---|---|---|
| *ADD3* | F: GGCTCTGCGGCGCTTA<br>R: CTTGTTATCTCGCAGCGCG | NM_016824.4 |
| *AHNAK* | F: CTCGTCGCCGCCAGTAG<br>R: TCTCGGTCACAACCTGAGG | NM_001620.2 |
| *CDH1* | F: CACCACGGGCTTGGATTTTG<br>R: TGGGGGCTTCATTCACATC | NM_001317184.1 |
| *CDH2* | F: GCGTCTGTAGAGGCTTCTGG<br>R: GCAGTTGCTAAACTTCACATTGA | NM_001792.4 |
| *COL4A2* | F: GGATGGCTATCAAGGGCCTG<br>R: CTGGCACCTTTTGCTAGGGA | NM_001846.3 |
| *FN1 (MSF)* | F: CCCATCCAGTGGAATGCACC<br>R: GGTGGGATACTCACAGGT | NM_054034.2 |
| *GAPDH* | F: GGTCATCCATGACAACTTTGG<br>R: CCATCCACAGTCTTCTGG | NM_004792.2 |
| *GATA4* | F: CTCCTCTGCACATTGCTGTT<br>R: GTGTGGGGAGGCGTAGT | NM_002052.3 |
| *IGFBP1* | F: TTTAGCCAAGGCACAGGAGA<br>R: ATGGATGTCTCACACTGTCTG | NM_000596.2 |
| *MMP1* | F: AGTCCAGAAATACCTGGAAAAATAC<br>R: TTTTTCAACCACTGGGCCAC | NM_002421.3 |
| *NRP2* | F: CTGTGGGTCATCCGTGAGGAC<br>R: ATGGGTTCCATGCAGTTCTCCAG | NM_201266.2 |
| *PPIG* | F: CAATGGCCAACAGAGGGAAG<br>R: CCAAAAACAACATGATGCCC | NM_004792.2 |
| *RHOB* | F: GTGTGTCTGTTCGACTCCCC<br>R: AGGGATATCAAGCTCCCGC | NM_004040.3 |
| *RHOU* | F: TGCCGGACAGGATGAATTTGA<br>R: TGGGACAGTGGCATCGAAT | NM_021205.5 |
| *SRC* | F: CAGATTGTCAACAACACAGAGGG<br>R: CACGTAGTTGCTGGGGATG | NM_004040.3 |
| *SYTL2* | F: AGTGAAGGCTCGCAACGC<br>R: CACCTACCTCCGAGTCG | NM_032943.4 |
| *TIMP2* | F: CAGATGTAGTGATCAGGGCCAA<br>R: CCTTCTCAGGCCCTTTGAA | NM_003255.4 |

### 4.2 *In situ* hybridization (I)

RNAscope Multiplex Fluorescent Reagent kit (v2, #323100; ACDBio, Milano, Italy) was employed for RNA in situ hybridization target detection. Paraffin-embedded formalin-fixed samples (5 µm thick) were baked at 60 °C for 1 h and then deparaffinized followed by hydrogen peroxidase treatment (10 min at RT). Target retrieval was carried out at +97 °C for 15 min and subsequently samples were treated with protease at +45 °C for 15 min. Probe hybridization (*GATA4* #579821) was performed at 40 °C for 2 h followed by signal amplification. Following fluorophores (PerkinElmer) were used at 1:1500 dilution for each: TSA Plus Cyanine 3 (NEL744001KT) and TSA Plus Cyanine 5 (NEL745001KT). DAPI was used to counterstain the sections.

Images were captured with 3DHISTECH Panoramic 250 FLASH II digital slide scanner at Genome Biology Unit (Research Programs Unit, Faculty of Medicine, University of Helsinki Biocenter, Helsinki, Finland).

### 4.3 RNA microarray (I)

HUH6 cells were transfected with *GATA4* or NT control siRNA and incubated for 72 h. RNA was extracted (Nucleospin RNA/Protein kit) and subsequently purified (Nucleospin RNA Clean-up XS kit, Macherey-Nagel) for the further processing. Two set of samples were collected from different passages (3+3 in each group). RNA quality was measured with Bioanalyzer (Agilent, CA, USA) and following all the samples were hybridized on Illumina Human HT-12 v4 oligonucleotide expression BeadChip (Illumina, San Diego, CA, USA) at Functional Genomics Unit (University of Helsinki). Background corrected raw data processed with BeadStudio software (Illumina) was quantile normalized and log transformed utilizing BedArray Bioconductor package (140). Differentially expressed genes were identified with LIMMA tool (141) with Benjamini-Hochberg correction and filtered by cut-off criteria false discovery rate (FDR) < 0.05 and lg2 fold change (FC) ± 0.2.

### 4.4 RNA sequencing data analysis (I, II)

Datasets with accession numbers as follows were downloaded from GEO database of National Center for Biotechnology Information (142) or EGA European Genome-phenome Archive (https://ega-archive.org/): GSE83518 (HUH6), EGAS00001004827 (HB-243, HB-279, HB-282, HB-284, HB-303), and GSE140520 (primary hepatocytes). Data was pre-processed utilizing Trimmomatic (143) and following aligned with reference genome (Homo_sapiens.GRCh38.9) using HISAT2 tool (144). Differentially expressed genes were identified employing edgeR package (145) and then filtered using cut-off criteria false discovery rate (FDR) < 0.05 and lg2 fold change ±1 .

### 4.5 RT$^2$ Profiler death pathway finder array (III)

Expression of 84 death signaling associated genes was explored utilizing RT$^2$ Profiler death pathway finder array (330231/PAHS-212ZA; Qiagen, Valencia, CA, USA) following manufacturer's instructions. Data was analyzed with GeneGlobe software

(Qiagen) and geometric mean of *B2M*, *HPRT1*, and *GAPDH* was used to normalize gene expression.

## 5 Protein expression analysis

### 5.1 Protein extraction and western blotting (I, II, III)

Total protein was isolated using the Nucleospin RNA/Protein kit (Macherey-Nagel). Proteins were separated with electrophoresis utilizing Mini-Protean TGX Stain-Free Gels (Bio-rad, Hercules, CA, USA) and transferred to PVDF membrane. Non-specific binding was blocked with 5 % fat-free milk in Tris-buffered saline with Tween 20. Primary antibody incubations were carried out at +4 °C for overnight and secondary antibody incubations were performed at room temperature for 1 h. Protein bands were visualized utilizing Enhanced Chemiluminescence detection kit (Amersham ECL reagent; GE Healthcare, Barrington, IL). Band intensities were normalized to the total protein amount in the corresponding lane exploiting Stain-free technology (146). Quantification was carried out with ImageLab software (version 6.0.1; Bio-Rad).

### 5.2 Immunohistochemistry (I, II)

Paraffin-embedded formalin-fixed patient samples in 5-µm sections were deparaffinized, hydrated, and then treated with target retrieval solution for 35 min at +98 °C (pH 9; Dako, Glastrup, Denmark). Hydrogen peroxidase (3 %) was used to avert endogenous peroxidase activity and 0.4 % casein was utilized to block unspecific binding (both solutions from Novolink Polymer Detection System Kit; Leica, Newcastle, UK). Primary antibodies were incubated either at room temperature for 1 h (NRP1) or at +4 °C for overnight (NRP2, GATA4). Novolink Polymer (Leica) and DAB substrate (Vector laboratories, Burlingame, CA, USA) were used to visualize protein expression. Primary antibody was replaced with non-immune serum in control experiments. Scoring was performed by two independent investigator. Antibody details are described in **Table 5**.

Images were captured with 3DHISTECH Panoramic 250 FLASH II digital slide scanner at Genome Biology Unit (Research Programs Unit, Faculty of Medicine, University of Helsinki Biocenter, Helsinki, Finland).

### 5.3 Immunofluorescence (I, II, III)

Cells were cultured on Matrigel or collagen I coated chamber slides for immunofluorescence experiments. For basic immunofluorescence staining, cells were fixed and permeabilized with ice-cold methanol. Unspecific binding was blocked with UltraVision Protein Block solution (Thermo Fisher Scientific). Primary antibody incubations were carried out at room temperature for 1 h. Next, samples were incubated with secondary antibody for 1 h in the dark. Mounting was performed with DAPI containing mounting medium to counterstain the nuclei.

Phalloidin staining was carried out per manufacturer's instructions. Briefly, cells were fixed with 4 % paraformaldehyde (PFA), permeabilized with Triton-X, and incubated

with UltraVision Protein Block Solution (Thermo Fisher Scientific). Antibody incubation was performed at room temperature for 1 h and samples were protected from light during the experiment.

Imaging was aquired with Zeiss Axio Imager M2 (Carl-Zeiss, Oberkochen, Germany). Detailed information of antibodies is given in **Table 5**.

**Table 5. List of antibodies.**

| Antibody | Host/source | Cat.no | Manufacturer | Method (concentration) |
|---|---|---|---|---|
| Anti-mouse IgG-Alexa488 | donkey | A21202 | Life Technologies | IF (1:200) |
| Anti-rabbit IgG-Alexa647 | goat | A32733 | Invitrogen | IF (1:500) |
| Anti-mouse IgG | goat | 115-005-062 | Jackson ImmunoResearch | WB (1:10 000) |
| Anti-rabbit IgG | goat | 111-005-045 | Jackson ImmunoResearch | WB (1:10 000) |
| GATA4 | mouse | AF2606 | R&D Systems | IF (1:150) IHC (1:5000) WB (1:500) |
| E-cadherin | mouse | 610181 | BD Transduction laboratories | IF (1:50) WB (1:1000) |
| N-cadherin | mouse | 610920 | BD Transduction laboratories | IF (1:200) WB (1:1000) |
| NRP1 | rabbit | ab81321 | Abcam | IHC (1:3000) WB (1:1500) |
| NRP2 | mouse | sc-13117 | Santa Cruz | IHC (1:2000) WB (1:800) |
| PARP1 | rabbit | 9532 | Cell Signaling Technologies | WB (1:1500) IF (1:800) |
| PARP2 | mouse | NBP2-47337 | Novus Biologicals | WB (1:1000) |
| Phalloidin-FITC | Amanita phalloides | P5282 | Sigma Aldrich | IF (1:250) |

**IF=immunofluorescence. IHC=immunohistochemistry. WB=western blotting.**

## 6 Functional studies

### 6.1 Cell viability (II, III)

Cell viability was assessed with two methods: tetrazolium salt-based WST-1 reagent (Roche Molecular Biochemicals, Mannheim, Germany) and ATP-based assay (PerkinElmer, Waltham, MA, USA). Cells were incubated with WST-1 reagent for 2 h and absorbance was measured at 450 nm with Multiskan FC Plate reader (Thermo Fisher Scientific). For ATP measurements, cells were lysed and incubated with ATP substrate

following manufacturer's instructions. Luminescence was metered with Enspire Multimode Plate reader (PerkinElmer).

**6.2 Clonogenic assay** (III)

Cells were plated at low density 24 h prior the chloroquine treatment initiation. Treatments were replaced daily and in the end of experiment cells were stained with crystal violet. Plates were imaged with ChemiDoc XRS+ Imaging System (Bio-Rad) and number of colonies was determined with ColonyArea Plugin in ImageJ (147).

**6.3 Caspase activity assay** (III)

Amount of apoptosis effector proteins caspase 3 and 7 (Caspase 3/7 Glo, Promega) were measured to assess the activation of apoptotic process. Cells were incubated with caspase 3/7 substrate for 2.5 h and luminescence was measured with Enspire Multimode Plate reader (PerkinElmer).

**6.4 Migration studies** (I, II)

Cell migration was evaluated with two different methods. For the wound healing assay (I), cells were cultured as a confluent monolayer on collagen I coated 6-well plates. A wound was made with 120 µl pipette tip and medium was replaced after scratching. Imaging was performed at the initiation and after 24h. The velocity of migratory front was calculated with ImageJ software (148).

Transwell assay (I, II) was performed utilizing migration inserts (pore size 8 µm; Merck Millipore, Darmstedt, Germany) placed into 24-well plates. Bottom of each insert was pre-coated with collagen I. Cells were seeded into inserts in serum-free medium and outside of the insert was normal cell culture medium. Cell were allowed to migrate for 40-42 h after which the inserts were fixed with PFA, permeabilized with 100 % methanol, and stained with crystal violet. Five randomly chosen fields of each insert were imaged and number of migrated cells was counted utilizing ImageJ (148).

**7 Chloroquine administration** (III)

Chloroquine diphosphate (CQ, ab142116; Abcam) was dissolved in sterile water as 10 mM stock solution. Further dilutions (1 µM, 5 µM, and 10 µM) were prepared in the adequate cell culture medium. CQ was administrated for 4-14 days an experiment-dependent manner and treatments were refreshed daily. Cell culture medium without CQ was used as a control treatment.

**8 Metabolism studies**

**8.1 Metabolomic profiling** (III)

Cell pellets (1.5 x $10^6$ cells/sample) were snap-frozen in liquid nitrogen and subjected to metabolomic profiling utilizing Acquity UPLC-MS/MS system and XEVO TQ-S Triple Quadrupole LC/MS system (Waters Corporation, Milford, MA, USA). Web-

based software MetaboAnalyst 4.0 (http://www.metaboanalyst.ca) (149) was employed to analyze normalized concentrations of 100 metabolites.

**8.2 Aspartate rescue experiment** (III)

Cells were treated either with 5 µM CQ, 10 mM aspartic acid (Sigma Aldrich), CQ + aspartic acid, or with control treatment. Cell viability after 96 h treatment period was assayed with ATPlite kit (Perkin Elmer) and luminescence was measured with Enspire Multimode Plate reader (Perkin Elmer).

**8.3 NAD/NADH assay** (III)

NAD/NADH assay kit was obtained from Abcam. HUH6 cells were cultured with or without CQ and after 96 h they were lysed. Processing was performed as described in (150) and samples were incubated for 1.5 h at room temperature. Absorbance was measured with FC Multiskan Microplate reader (Thermo Fisher Scientific). Normalized concentrations were utilized to calculate NAD/NADH by equation ([NADtotal—NADH])/[NADH].

**9 Statistical analyses**

Three independent experiments were carried out for all the *in vitro* experiments if otherwise has not stated. Student's t-test or ANOVA followed with Dunnet's test was utilized to assess statistical significancy. Statistical significancy was set to p-value < 0.05. For RNA sequencing and mRNA microarray, statistical methodology is described in corresponding chapter (see above).

# RESULTS AND DISCUSSION

## 1 GATA4 as a regulator of epithelial-mesenchymal transition in hepatoblastoma cells (I)

### 1.1 GATA4 expression in HB patient samples and cell lines

Aberrant activation of developmental pathways is a well-recognized feature of HB molecular pathogenesis (reviewed in 9). Transcription factor GATA4 is crucial for early liver development and its abnormal expression has been linked to pro-tumorigenic processes in several cancer types (152–154).

An earlier study by Soini et al. demonstrated that GATA4 is abundantly expressed in HBs (155), but its role in HB pathogenesis has not been fully clarified. In this study we confirmed GATA4 expression in HBs using additional methodology and larger sample set (n=24) that was included in the previous study. RNA in situ hybridization demonstrated *GATA4* mRNA expression in HB cells while low or negligible amounts were detected in the healthy hepatocytes (**Figure 9A, C**). At the protein level, GATA4 expression was restricted to Kupffer cells and LSECs in the normal liver (NL) which is consistent with previous findings (155,156). Most HBs (83 %) showed moderate or high GATA4 protein expression localizing especially to embryonal areas of the tumor (**Figure 9D**) whereas 17 % of samples had low or negative GATA4 immunoreactivity. We did not observe any correlation between GATA4 expression and PRETEXT stage though the number of patients in each group was relatively low to reach statistical power (PRETEXT II n=7, PRETEXT III n=9, PRETEXT IV n=8).

RNA sequencing data analysis revealed *GATA4* overexpression in 5 PDX-derived HB cell lines, 4.1-8.2 -fold increase compared to primary hepatocytes, respectively (Eloranta et al., unpublished data, **Figure 9E**). Similarly, high GATA4 expression has been observed in immortalized HB cell model HUH6 (157,158).

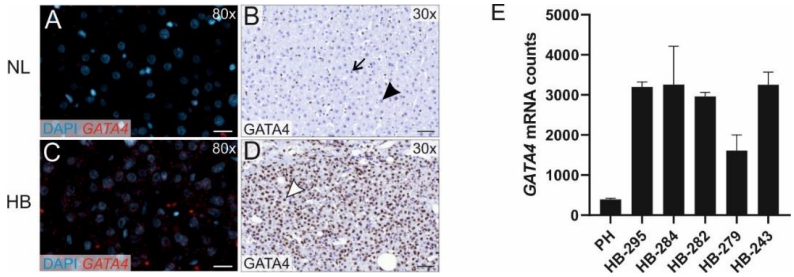


**Figure 9. GATA4 expression in HB tissue samples and PDX-derived cell lines.** *RNA in situ hybridization and IHC showing localization of GATA4 in NL (A-B) and HB (C-D). Arrow indicates GATA4 positive Kupffer cells in NL and black arrowhead points out GATA4 negative healthy hepatocytes (B). White arrowhead shows nuclear GATA4 expression in HB (D). RNA-sequencing demonstrated overexpression of GATA4 in HB cell lines (E). PH=primary hepatocyte. Scale bar: 100 µm (A-D).*

### 1.2 RNA interference mediated *GATA4* silencing in HB cells

GATA4 upregulation has been associated with tumor cell plasticity, increased chemoresistance, escape from programmed cell death, and proliferative phenotype in cancer cells (152,154,157). Based on these observations, we hypothesized that extensive GATA4 expression promotes malignant behavior in HB. To elucidate mechanisms by which GATA4 acts in HB pathogenesis, the immortalized HUH6 cell line was transfected with *GATA4* or non-targeting control siRNA. With this method, *GATA4* expression decreased approximately 80 % at the mRNA level **(Figure 10A**). A drastic decrease in GATA4 immunoreactive nuclei was also observed indicating that gene silencing leads to reduced protein expression (**Figure 10B-E**).

At the time this study was carried out, the number of commercially provided HB cell models was extremely limited. Thus, *in vitro* experimentations were conducted mainly utilizing HUH6 cell line representing mixed epithelial subtype of HB. Considering the broadly heterogenous nature of HB, GATA4 may have dissimilar roles in different HB subtypes limiting the applicably of results in this study. Furthermore, tumors are composed of variety of cell types and interactions between tumor cells and microenvironment cannot be mimicked in traditional cell cultures.

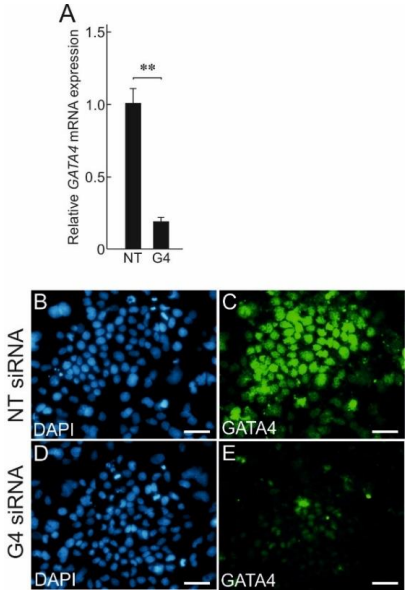


**Figure 10. GATA4 silencing in HUH6 cell line.** *RNA interference mediated gene silencing decreased GATA4 expression approximately 80 % at the mRNA level measured with RT-qPCR (A). GATA4 mRNA expression is a mean ± SD of three independent experiment and represented as a relative value (**p-value<0.01). HUH6 cells treated with NT control siRNA demonstrated strong nuclear GATA4 expression (C). GATA4 intensity and number of positive cells decreased drastically after GATA4 knockdown (E). DAPI was utilized as a nuclear counterstain (B, D). Scale bar: 20 µm (B-E). NT=non-targeting siRNA. G4=GATA4 siRNA.*

### 1.3 Global transcriptomic changes after *GATA4* silencing in HB cells

To explore global gene expression alterations associated with GATA4 in HB, we carried out an mRNA microarray hybridization on HUH6 cells with intact or silenced *GATA4* expression. Samples were collected from two different passages (3+3 / group) to minimize biases caused by transformation during passaging. Genes which were differentially expressed in both sample sets were included in the further analysis. We observed 106 differentially expressed genes (filtered by adjusted p-value < 0.05, lg2 FC± 0.2) in *GATA4* silenced cells versus NT siRNA treated cells of which 72 were downregulated and 34 were upregulated (**Figure 11**).

Surprisingly, the magnitude of single gene alterations was relatively small (fold changes were between 0.5-1.45). Based on animal studies, it has been suggested that GATA6 could compensate partial loss of GATA4 during the early liver development (3,159). In addition to GATA4 upregulation, aberrant GATA6 expression has been reported in HBs (155). If GATA6 is partially regulating same target genes than GATA4 in HUH6 cells, this may explain why we did not observe more drastic changes in the global transcriptome.

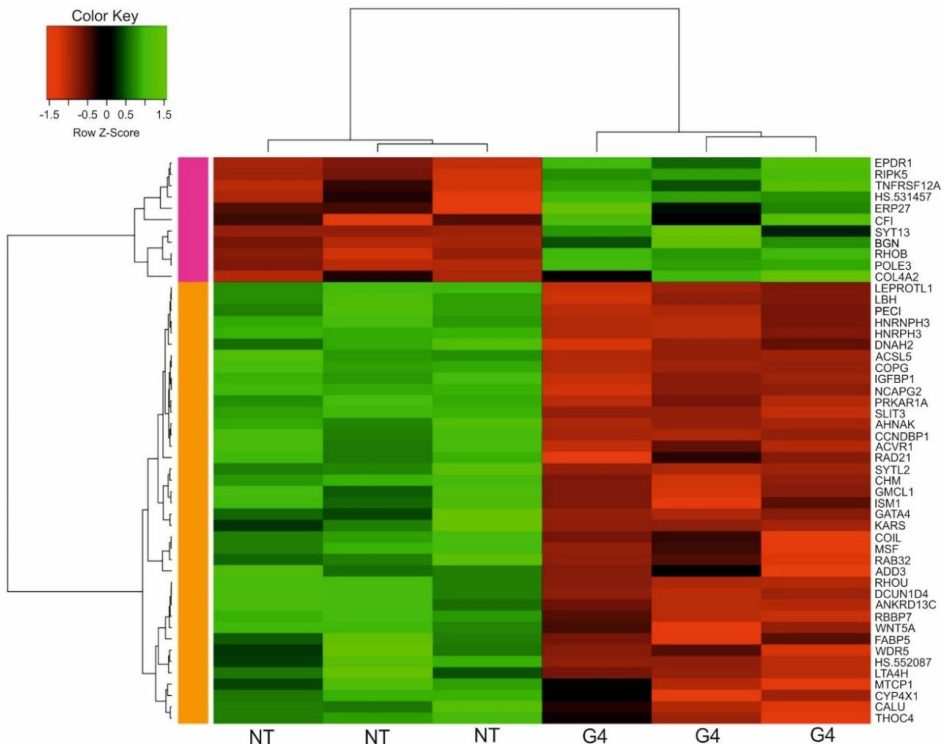


**Figure 11. Differentially expressed genes (top 50) 72 h after *GATA4* silencing in HUH6 cells.** *Results are filtered by adjusted p-value (<0.05) and clustered utilizing 2-dimensional hierarchical clustering approach. NT=non-targeting siRNA. G4=GATA4 siRNA.*

## 1.4 Over-representation of epithelial-mesenchymal transition associated genes in *GATA4* knockdown HB cells

Computational gene ontology (GO) enrichment analysis (160) highlighted abundancy of the gene sets related to developmental processes, cell adhesions, motility, or polarity (**Figure 12**) in microarray of *GATA4* silenced cells. All the aforementioned biological processes are associated with epithelial-mesenchymal transition (EMT) [reviewed in (161)].

EMT is a dynamic and reversible process that converts stationary polarized epithelial cells to motile mesenchymal cells. In brief, through genetic re-programming epithelial cells gradually lose apico-basal polarity and cell-to-cell junctions, re-organize the cytoskeleton, and adjust extracellular matrix composition to support migration and invasion in transformed mesenchymal cells (162). Physiologically, EMT plays important part in the early embryonic development and later it occurs during the wound healing. In the context of cancer, EMT facilitates malignant progression by enabling tumor cells to spread and invade from the original location to surrounding areas and subsequently occupy distant sites [reviewed in (163)].

Taken together, considering the role of GATA4 during the embryogenesis, GATA4 overexpression may maintain aberrant activation of developmental processes, such as EMT, as suggested by our data. This observation is also supported by recent study linking GATA4 overexpression with EMT-related genes and processes in nasopharyngeal cancer (152).

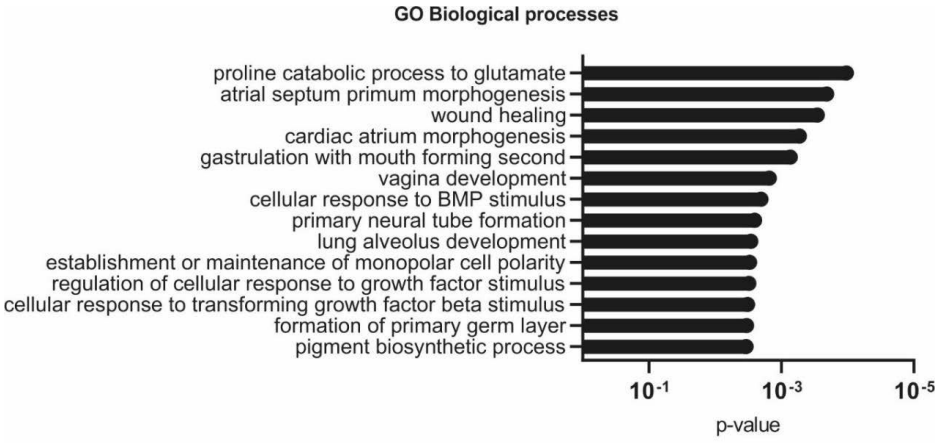


**Figure 12**. **Enriched biological processes in microarray data of GATA4 silenced HUH6 cells.** *Biological processes relating to ontogenesis, wound healing, cell polarity, and response to the stimulus were among the top 10 of most altered processes in the gene ontology (GO) analysis.*

## 1.5 GATA4 contributes to modification of cytoskeleton architecture and cell adhesions

To validate differentially expressed genes in the mRNA microarray, we assayed EMT-associated genes with RT-qPCR in two HB cell lines. Additionally, we evaluated expression of E-cadherin (*CDH1*), N-cadherin (*CDH2*), proto-oncogene c-Src (*SRC*), matrix metalloproteinase 1 (*MMP1*), and tissue inhibitor of metalloproteinases 2 (*TIMP2*) which were not initially noted in the microarray but are hallmarks of EMT (164–166). Seven of the studied genes were associated with cell motility or cytoskeleton rearrangements, two were related to apico-basal polarity and cell adhesions, and four genes were connected to remodeling of extracellular matrix. In HUH6 cells gene expression was changed to same direction than it was observed in array, but all the results were not consistent with HepG2 HB cell line (Table 6). The HepG2 cell line was originally derived from an older (15 years) HB patient compared to HUH6 cells representing HB in infant. HB pathogenesis is likely partially different in older HB

patients, but it has not been widely studied if there is for example higher mutation burden in this group compared to younger HB patients. In sum, GATA4 seems to regulate multiple genes involved EMT-related processes, but exact mechanism may be environment dependent. To elucidate whether all or some of the genes studied here are under direct transcriptional control of GATA4 in HB cells, chromatin-immunoprecipitation assay (167) should be utilized in the future studies.

**Table 6. Gene expression of EMT-associated genes after *GATA4* silencing measured with RT-qPCR.**

| Gene symbol | HUH6 G4/NT ratio* | HepG2 G4/NT ratio* | EMT-associated function | Reference |
|---|---|---|---|---|
| *ADD3* | 0.73 | 1.50 | cell motility and cytoskeleton rearrangements | (168) |
| *AHNAK* | 0.61 | 0.72 | cell motility and cytoskeleton rearrangements | (169) |
| *CDH1* | 1.47 | 2.20 | cell-to-cell adhesions and apico-basal polarity | (170) |
| *CDH2* | 0.71 | 1.39 | cell-to-cell adhesions and apico-basal polarity | (171) |
| *COL4A1* | 1.46 | ns | extracellular matrix remodeling | (172) |
| *DOCK8* | 0.71 | ns | cell motility and cytoskeleton rearrangements | (173) |
| *IGFBP1* | 0.51 | 0.70 | extracellular matrix remodeling | (174) |
| *MSF* | 0.57 | ns | extracellular matrix remodeling | (175) |
| *MMP1* | 0.46 | 2.37 | extracellular matrix remodeling | (166) |
| *RHOB* | 1.46 | 1.55 | cell motility and cytoskeleton rearrangements | (176) |
| *RHOU* | 0.69 | ns | cell motility and cytoskeleton rearrangements | (177) |
| *SRC* | 0.77 | 1.26 | cell motility and cytoskeleton rearrangements | (165) |
| *SYTL2* | 0.48 | ns | cell motility and cytoskeleton rearrangements | (178) |

*=p-value < 0.05. ns=not significantly differentially expressed.

Cadherin-switch is an EMT-related process wherein E-cadherin is downregulated and N-cadherin is upregulated enabling changes in cell polarity (179). A prior study in canine kidney cells showed that *CDH1* is directly upregulated by GATA4 (170). We observed reversed cadherin-switch after *GATA4* silencing both in our gene expression analysis and immunofluorescence staining (**Table 6**, **Figure 13C-F).** A shift towards E-cadherin dominancy supports epithelial and less-motile phenotype. Knockdown of *GATA4* also reduced actin polymerization and stress fiber accumulation in HUH6 cells **(Figure 13A-B**) suggesting that GATA4 is involved in both the regulation of cell junction dynamics and cytoskeletal remodeling in HB.

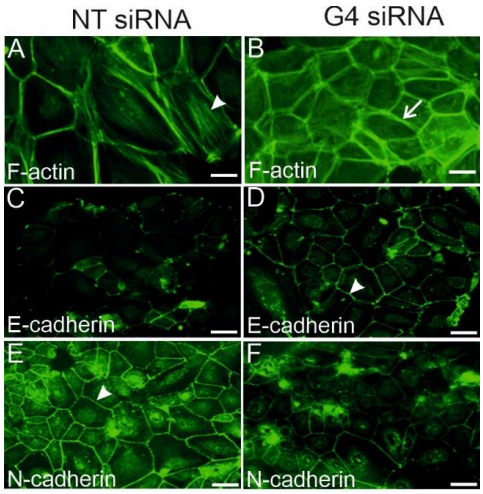


**Figure 13. Immunofluorescence staining of EMT markers.** *Stress fibers (arrowhead) accumulated in HUH6 cells with intact GATA4 expression (A). After GATA4 silencing, membranous actin (arrow) was more prominent (B). F-actin was stained with phalloidin (A, B). GATA4 knockdown upregulated E-cadherin expression in HUH6 cell membranes (arrowhead) (C-D). N-cadherin was predominant in membranes (arrowhead) of cells treated with NT siRNA (E-F). Scale bar 50 µm (A-G). NT=non-targeting. G4=GATA4.*

### 1.6 *GATA4* silencing reduces cell migration

Rearrangement of adhesion and cytoskeletal proteins is a prerequisite for cell migration and invasion (180). We found that cells with undisturbed GATA4 expression were remarkably more mobile (**Figure 14A-B, E**) than those treated with *GATA4* siRNA (**Figure 14C-E**). Similar findings were presented in study by Pei et al., who showed that upregulated GATA4 increased migration and invasion in HUH6 HB cells by regulating expression of microRNA-125b (miR125b) and DKK3 (158). However, our microarray analysis did not detect alteration in DKK3 expression after *GATA4* silencing in the same cell line. Microarrays have been criticized for inaccuracies (181) which may explain this discrepancy, but further studies are needed to conclude significance of GATA4-DKK3 axis. Small non-coding RNAs were not included in the microarray used.

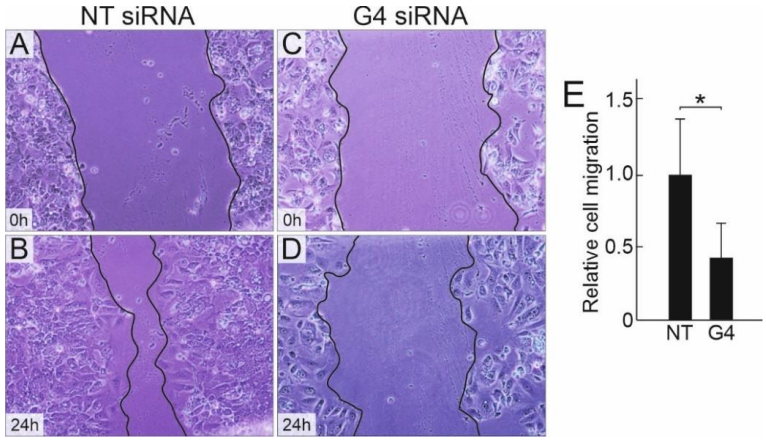


**Figure 14. Motility of HUH6 cells after *GATA4* silencing.** *Migration pace was 2.6-fold (E) higher in cells with undisturbed GATA4 expression (A-B) compared to GATA4 knockdown cells (C-D) at 24 h timepoint. Black line demonstrates the cell front (A-D). Mean of three experiments ± SD is shown in bar plot (E). *p-value<0.05. NT=non-targeting. G4=GATA4.*

### 1.7 Overexpression of GATA4 in primary hepatocytes

Since we observed that GATA4 silencing modifies EMT-related gene expression, we next explored whether GATA4 overexpression shifts normal hepatocytes towards a malignant phenotype. To test this, GATA4 expression was enforced in human primary hepatocytes (PH) from adult donor. Low baseline expression of GATA4 was detected in PH (HUH6/PH *GATA4* mRNA ratio 0.23, p-value 0.002). Following plasmid transfection, *GATA4* expression increased 229-fold. Utilizing RT-qPCR, we investigated expression of EMT-related genes after enforced GATA4 upregulation. Most of these genes (10/14) were significantly altered (**Figure 15A-C**). Furthermore, 8/10 were changed to opposite direction than in *GATA4* silenced HUH6 cells suggesting that GATA4 is able to modify gene expression of differentiated hepatocyte towards mesenchymal cell type. It is noteworthy that the baseline of *GATA4* mRNA expression was approximately four times higher in HUH6 cells compared to PH. Enforced overexpression resulted remarkably higher *GATA4* mRNA expression in PH than the aforementioned baseline. Actions of GATA4 may differ dose-dependent manner and this should be noted when evaluating these results.

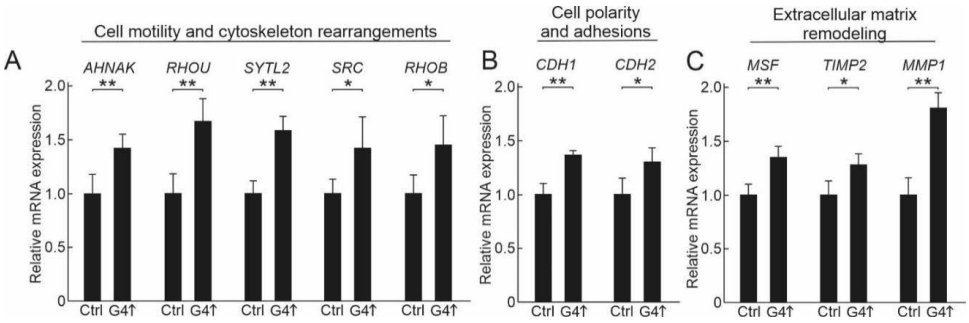


**Figure 15. Gene expression changes in primary hepatocytes after enforced GATA4 expression.** *Five genes (5/7) associated with cell motility and cytoskeleton rearrangements were upregulated after transfection with GATA4 expression plasmid (A). GATA4 upregulated both CDH1 as well CDH2 expression in primary hepatocytes (B). Three genes (3/4) linked to extracellular matrix remodeling were altered by upregulated GATA4. Experiment was performed in triplicate and bar plots indicate relative mean ±SD. *=p-value<0.05. **p-value<0.01. G4=GATA4 expression plasmid. Ctrl=control plasmid.*

Altered GATA4 expression has also been demonstrated in the adult form of HCC, but interestingly it has been suggested to have tumor suppressor role in this cancer type (182). Of note, the etiology of adult HCC differs from HB, as HCC often manifests in inflamed or injured liver. This observation underlines the idea that GATA4 actions in liver might be dependent on other molecular events, such as inflammation or ontogenesis, occurring simultaneously with tumorigenesis.

### 1.8 Summary of the findings related to GATA4 in HB

Transcription factor GATA4 is highly expressed in HBs and this is especially evident in tumors with embryonal histology. Additionally, excessive *GATA4* expression was observed in HB cell lines. Using RNA interference based methodology, *GATA4* was silenced and its impact on global transcriptome was assessed. We noted that high proportion of altereted genes were associated with EMT-related processes. Further, we observed that the phenotype of *GATA4* silenced HB cells shifted towards epithelial and immobile cell as the E/N-cadherin ratio turned around and number or migratory cells decreased. Enforced GATA4 expression in primary hepatocytes was able to modify gene expression towards that of characteristic for HB. Taken together, GATA4 associates with mesenchymal-like phenotype in HUH6 cells and its silencing leads to reduction of malignant behaviour of HB cells. It has to be noted, however, that all the experimentations were conducted in simple cell models and actions of GATA4 might be different in a complex tumor environment *in vivo*.

# 2 Neuropilin expression in hepatoblastoma HB (II)

## 2.1 Neuropilin-2 expression in HB patient samples and cell lines

Neuropilins (NRP1 and NRP2) are non-tyrosine kinase receptors with plethora of ligands expressed both in physiological as well pathological situations (183–185). In cancer cells, upregulation of NRPs has been associated with several pro-malignant processes including chemoresistance, increased viability, and metastatic behavior (99,186,187). Moreover, recent studies have demonstrated that NRP1 and NRP2 may serve as diagnostic and prognostic markers in liver carcinoma (98,188).

To investigate the expression of NRPs in HB, we measured mRNA and protein levels in patient samples and HB cell lines. Consistent with prior studies (80,189), we did not observe considerable NRP1 or NRP2 expression in normal hepatocytes, whereas LSECs expressed both NRPs, providing an internal control (**Figure 16A-B**). All of HB patient samples (n=20) demonstrated NRP1 immunoreactivity, half of HBs (50 %) had low or intermediate expression (**Figure 16C**) and rest of the samples (50 %) showed high expression (**Figure 16E**). NRP2 was expressed in 95 % of HBs, 55 % of the samples had low or intermediate expression (**Figure 16D**) and 40 % of the samples had high NRP2 immunoreactivity (**Figure 16F**), respectively. One HB patient sample was NRP2 negative.

Patients included in this study formed subgroups of 2-8 subject in each based on major clinical variables such as staging, metastasis, and survival. This kind of data is extremely vulnerable to bias owing to the small sample size. For this reason, we opted not to correlate NRP expression with clinical variables in this study.

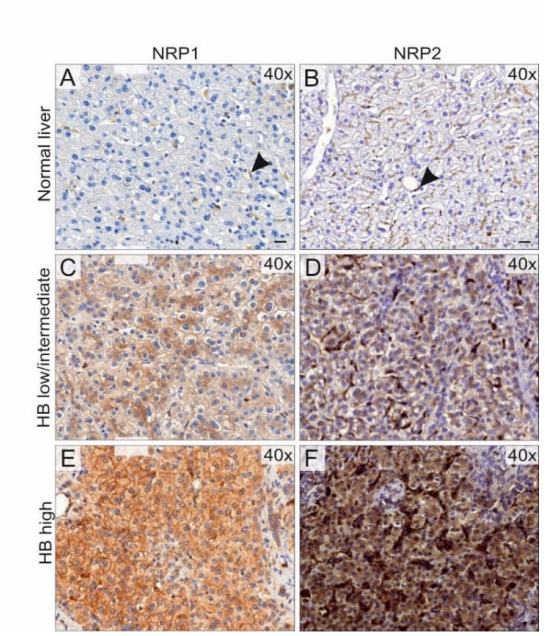


**Figure 16. NRP1 and NRP2 expression in normal liver and HB patient samples.** *Normal hepatocytes did not show considerable NRP1 or NRP2 expression whereas LSECs (arrow) were positive for both markers (A-B). NRP1 expression, 10/20 with low/intermediate intensity (C) and 10/20 with high intensity (E), localized to cytoplasm and membranes of HB cells. Intermediate/low NRP2 expression (D) was detected in 11/20 HBs and 8/20 HBs had high expression (F). NRP2 expression was detected predominantly in cytoplasm with lesser amounts in membranes (D, F). Scale bar = 20 µm. LSEC=liver sinusoidal endothelial cell.*

We also evaluated NRP1 and NRP2 expression in 6 HB cell lines. Primary hepatocytes were used as a control to detect baseline expression. At the mRNA level, significantly upregulated *NRP1* was detected in 4 of 6 six HB cell lines (**Figure 17A**) and similar expression was evident at protein level (**Figure 17B**). All HB cell lines demonstrated overexpression of *NRP2* at the mRNA level (**Figure 17C**). High NRP2 protein expression was observed in 5/6 HB cell lines, whereas one cell line had negligible expression like primary hepatocytes (**Figure 17D**).

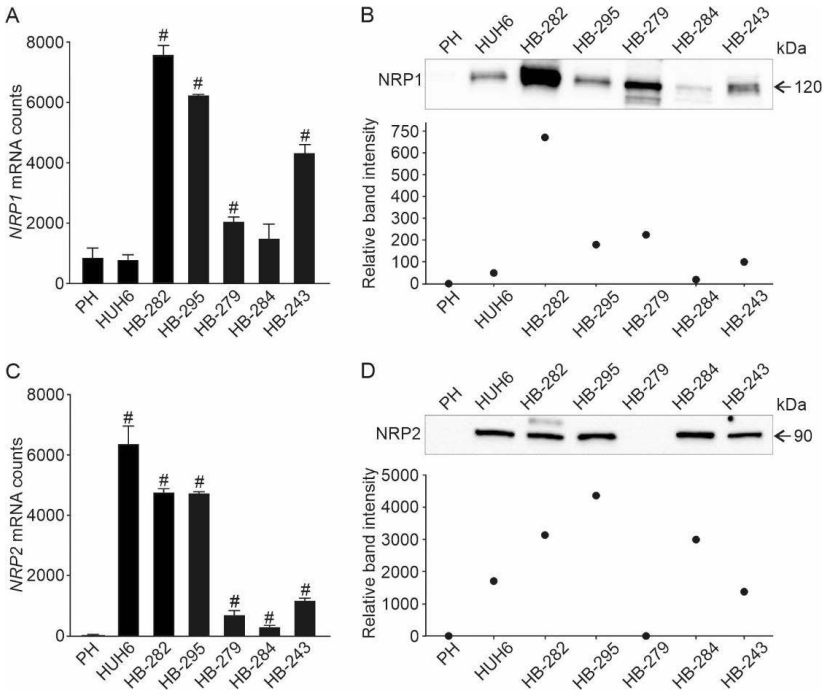


**Figure 17. NRP1 and NRP2 mRNA and protein expression in HB cell lines. Mean of** *NRP1 and NRP2 mRNA counts (±SD) measured with RNA sequencing (A, C) and protein expression (B, D) in HB cell lines and primary hepatocytes. Protein band intensities are normalized to total protein expression of the corresponding lane and relative band intensity describes expression in relation to primary hepatocytes (B, D). #=adjusted p-value<0.05. PH=primary hepatocyte.*

Interestingly, in the study by Wittman et al. NRP2 expression was linked to mesenchymal and dedifferentiated phenotypes in HCC (189). We observed abundant NRP2 expression in majority of HB patient samples and cell lines suggesting that NRP2 expression might be a common feature of poorly differentiated hepatic malignancies.

## 2.2 Knockdown of *NRP2* in HUH6 cells and its effect on cell viability

As NRP2 expression was consistently higher than NRP1 expression (1400- to 4300-fold vs. 70- to 700-fold ratio) in our HB cell models, we decided to focus on the role of NRP2 in HB pathobiology. We silenced *NRP2* expression in HUH6 cells and evaluated resultant changes in cell morphology and behavior. Utilizing siRNA transfections, we achieved approximately 70-80 % reduction in NRP2 expression (**Figure 18A-C**). Since the baseline expression of NRP2 was basically non-existent in primary hepatocytes, this remaining 20-30 % expression in HUH6 cells may still have a significant role in malignant processes. To overcome this, CRISPR-Cas9 genome editing technology (190), which enables complete inactivation of the gene, could be utilized in the future studies.

Aberrant NRP2 signaling has been associated with increased cell survival in variety of solid tumor models including breast, gastric, and cervical cancer cell lines (191–193). To investigate whether NRP2 affects also on HB cell viability, we assessed activity of mitochondrial dehydrogenases (WST-1) and ATP production. As with aforementioned cancer cell models, downregulation of NRP2 decreased HUH6 cell viability approximately 30% compared to cells with intact NRP2 expression (**Figure 18C-D**). In addition to other pro-survival effects, NRP2 overexpression was recently linked to cisplatin resistance in neuroblastoma cells (194). As cisplatin is a mainstay of HB chemotherapy, NRP2 targeting may also increase HB cell chemosensitivity.

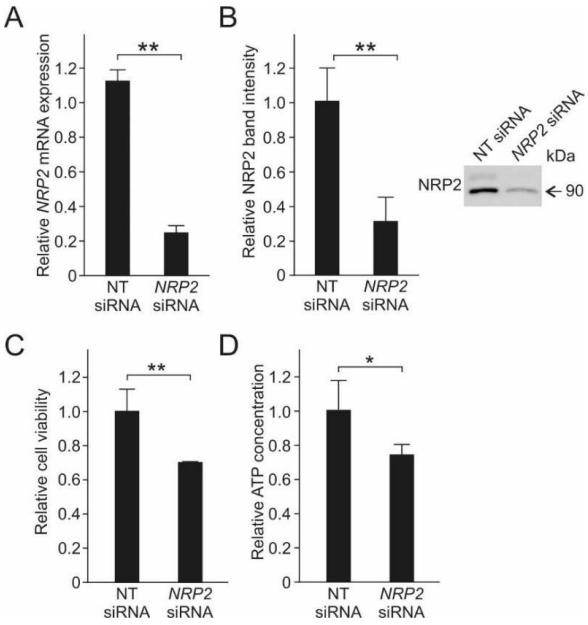


**Figure 18. *NRP2* silencing efficacy and impact on HUH6 cell viability.** *NRP2 expression decreased 70-80 % at mRNA (A) and protein (B) level. Band intensity was normalized to total protein expression of the corresponding lane utilizing stain-free technology (B). Cell viability measured with WST-1 (C) and ATP assays (D) after NRP2 knockdown. Bar plots are represented as a mean ± RSD of three independent experiments.*

## 2.3 Cytoskeleton remodeling and migration after *NRP2* silencing

NRP2 expression has been linked to stem-cell renewal and increased tumor cell motility in other pediatric and gastrointestinal cancers (189,192,195,196). To investigate if NRP2 contributes to similar processes in HB, we explored stress fiber formation and migration in HUH6 cells after *NRP2* knockdown. Re-organization of actin cytoskeleton is a prerequisite for tumor cell motility and subsequent metastasis [reviewed in (197)]. An essential part of this remodeling process is polymerization of actin fibers resulting in structures called stress fibers. These stress fibers further organize to form membrane protrusions that enable cell movements.

We noted a drastic decrease in actin stress fibers after *NRP2* silencing (**Figure 19D-F**) compared to cells with undisturbed *NRP2* expression (**Figure 19A-C**). Membrane

protrusions were more prominent in HUH6 cells with intact *NRP2* expression (**Figure 19A**) than in *NRP2* knockdown cells (**Figure 19D**).

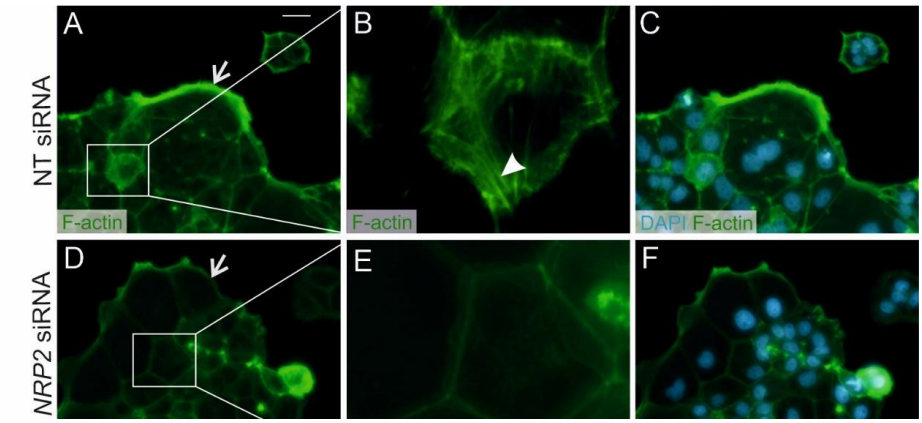


**Figure 19. F-actin staining in HUH6 cells with undisturbed or silenced *NRP2* expression.** *The white arrow indicates actin membrane protrusions in NT siRNA (A) and NRP2 siRNA treated HUH6 cells. Close-up of stress fibers (white arrowhead) (B-E). DAPI nuclear counterstaining merged with F-actin staining (C-F). Scale bar 50 µm.*

Since NRP2 expression in HB cells was associated with morphology promoting motility, we next assayed whether this correlates with actual migration rate. Using transwell assays, we noted that *NRP2* silencing (**Figure 20B**) led to a significant decrease in the number of migrated cells (**Figure 20C**) compared to HUH6 cells treated with NT control siRNA (**Figure 20A**). Considering the importance of cytoskeleton re-organization and motility for subsequent metastasis, targeting proteins crucial for these processes has potential in management of cancer. Antibodies blocking NRP2 activity have been investigated in pre-clinical cancer models with promising results (192,198). As current pharmaceutical treatment for HB is based on traditional chemotherapy associated with toxic side effects, targeted therapies such as anti-NRP2 antibodies may offer an additional novel tool to tackle these tumors.

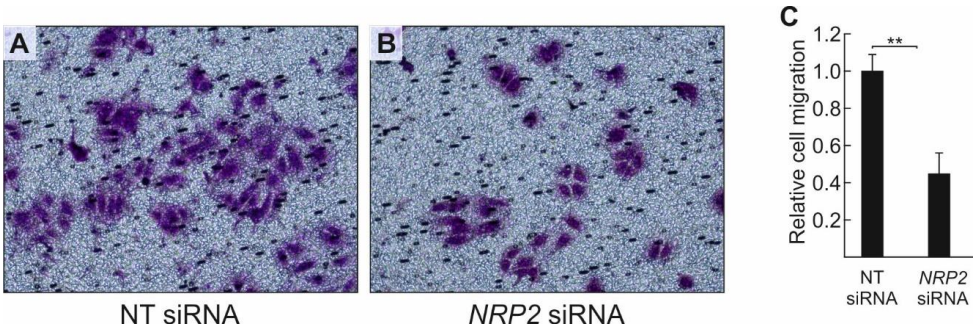


**Figure 20. Effect of NRP2 expression on cell motility in HUH6 cells.** *NRP2 silencing reduced cell motility (B) compared to cells treated with NT control siRNA (A). A 55 % decrease in the number of migrated cells were observed (C). Bar plot represents the mean of three independent experiment ± RSD. **p-value<0.01. NT=non-targeting.*

## 2.4 Summary of the findings related to NRP2 in HB

Both NRP1 and NRP2 are overexpressed in majority of HB patient samples and cell lines. RNA interference mediated silencing of *NRP2* attenuated HUH6 cell survival. Further, depolymerization of actin fibers was observed in NRP2 knockdown cells suggesting impaired mobility. This was confirmed with migration assay demonstrating significantly decreased motility of *NRP2* siRNA treated cells compared to control cells.

# 3 Pre-clinical evaluation of chloroquine in HB treatment (III)

## 3.1 HB cell viability after chloroquine treatment

Chloroquine is known to be a potent autophagy inhibitor. This is one of the principal mechanisms thought to underlie its efficacy in cancer treatment. Increased autophagy flux has been associated with multiple pro-tumorigenic processes such as altered DNA-damage repair and metabolomic reprogramming (199,200). In HB increased autophagic activity has been linked to tumor development in mice models (201). Based on that observation, we hypothesized that interventions targeting autophagy flux could be beneficial in HB management.

We established seven HB spheroid models (six PDX-derived cell lines and HUH6) and treated each with increasing concentrations of CQ (1 μM, 5 μM, and 10 μM). Remarkable changes in spheroid morphology indicative of decreased cell viability were observed in both a dose- and time-dependent manner (**Figure 21A-G**). Solid tumors typically contain differentially oxygenated and nourished areas. This phenomenon is recapitulated in spheroids - the outmost cells are typically proliferating, cells in the middle are quiescent, and interior cells are necrotic due to oxygen and nutrient deprivation (**Figure 21H**). This capability to mimick tumor architechture is a great advantage compared to traditional 2D monolayer cultures, though organoids would be even better to model complexity of tumor microenvironment.

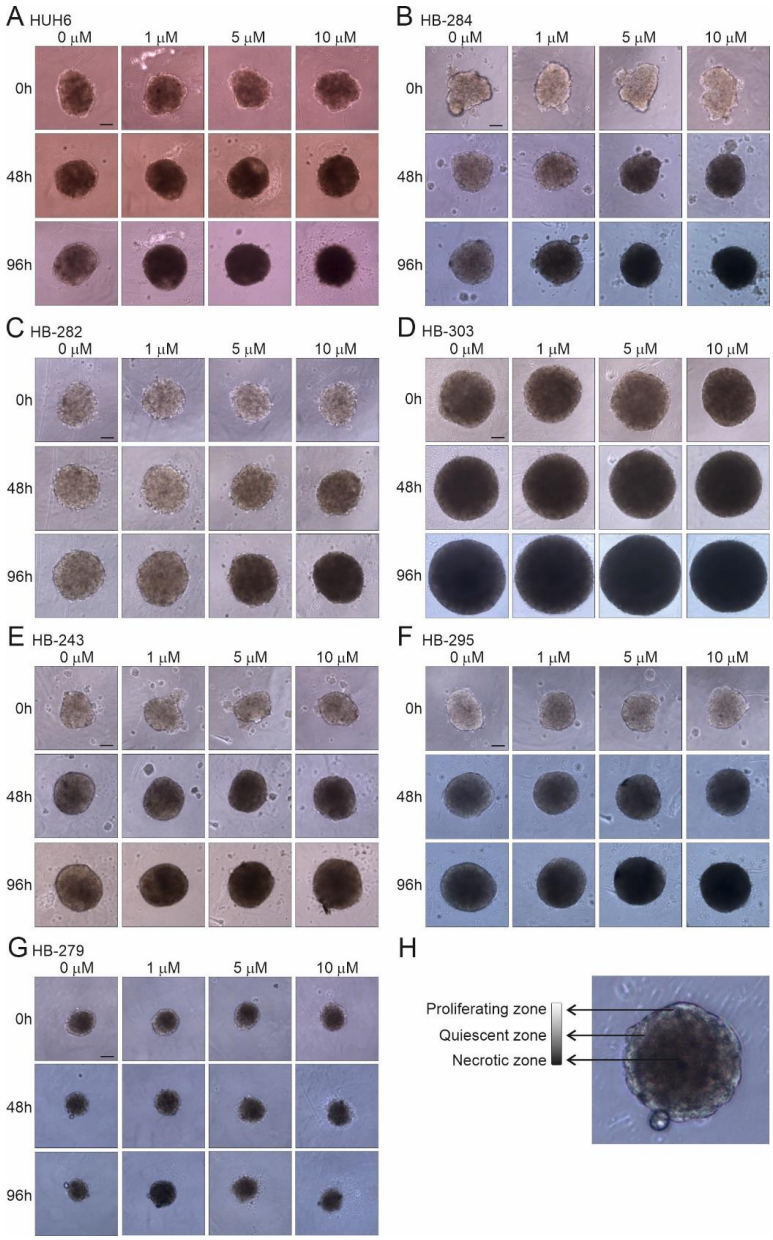


**Figure 21. HB spheroid morphology after 48 h and 96 h of CQ treatment.** *Light areas indicative of proliferating cells decreased in a time- and dose dependent manner in seven HB spheroid models (A-G). Representation of different zones in spheroid (H).*

To quantify the effect of CQ on HB cell viability, we measured ATP concentration and activation of apoptosis effector proteins caspase 3 and 7 after 48 h and 96 h of CQ treatment. At the 48 h timepoint, two out of seven models demonstrated decrease in ATP concentration and all the models exhibited increased apoptosis with 10 μM CQ concentration (**Figure 22A-G**). By 96 h, 6 of 7 HB spheroid models demonstrated significantly decreased viability (**Figure 22A-E, H**). Caspase 3/7 activation was even more pronounced in 4 of 7 models after 96 h of CQ treatment (**Figure 22A-C, E**). Consistent with our findings, CQ has demonstrated pro-apoptotic and anti-proliferative actions in various other cancer models (111,112,202).

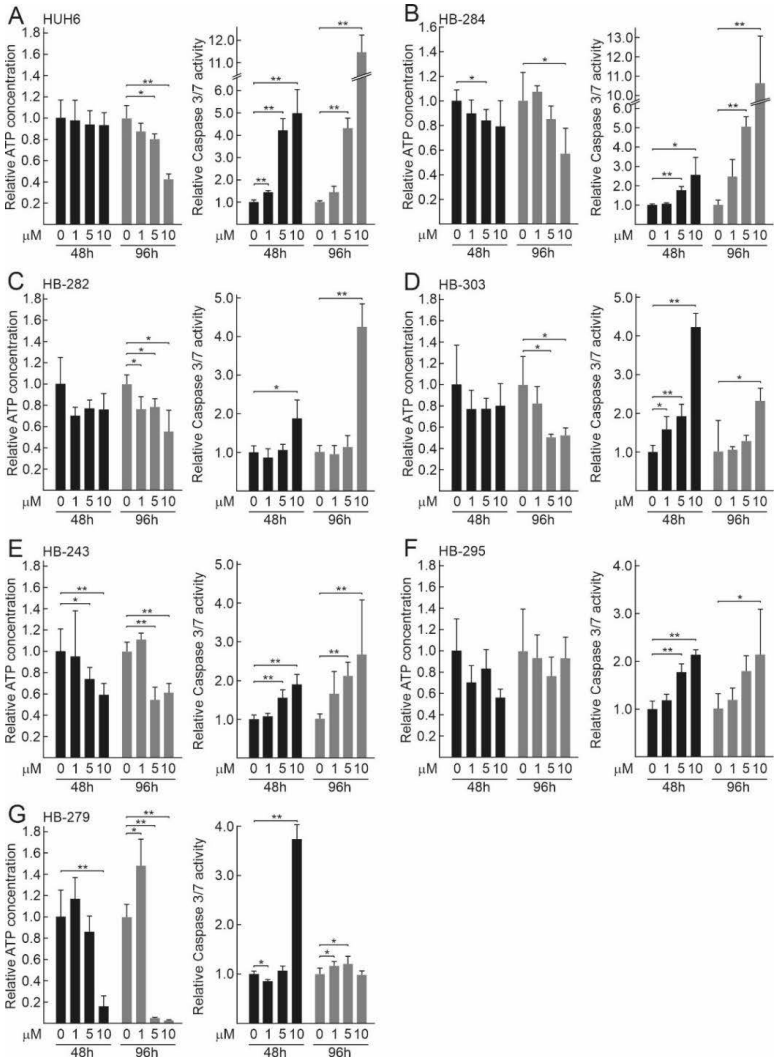


**Figure 22. Effect of CQ administration on HB spheroid viability and caspase 3/7 activation at 48 h and 96 h after treatment initiation (A-G).** **p-value < 0.05. **p-value < 0.01. CQ concentrations: 0 μM, 1 μM, 5 μM, and 10 μM.*

One major limitation of spheroid cultures is low cell density. Most high throughput applications require higher cell counts. Therefore, we validated spheroid findings in 2D cell cultures. We treated HB cell monolayers with fixed concentrations of CQ and measured clone formation potential after 4 d and 14 d of treatment. CQ (5-10 µM) had a statistically significant effect on clonogenic potential formation at both timepoints (**Figure 23A-C**).

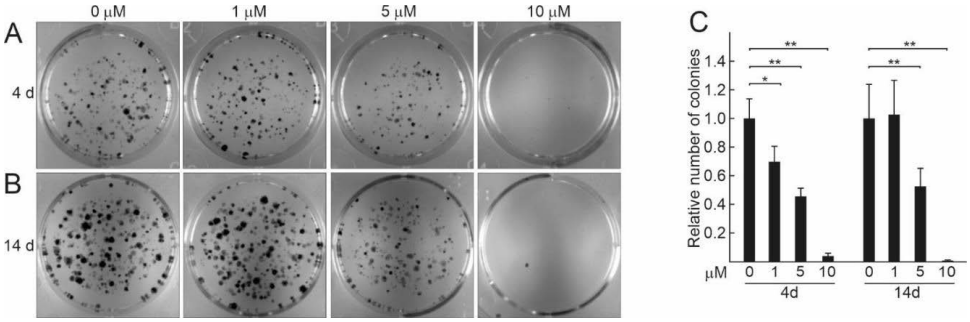


**Figure 23. Clonogenic potential in HUH6 2D cell cultures treated with CQ.** *After 4 days of treatment, the number of colonies decreased significantly with all the doses tested (A, C). Similarly, 5 µM and 10 µM doses reduced number of colonies after 14 d of treatment (B, C). CQ concentrations: 0 µM, 1 µM, 5 µM, and 10 µM.*

### 3.2 Metabolomic profile of chloroquine treated HUH6 cells

Disturbed autophagic flux has been associated with decreased nutrient availability in cancer cells [reviewed in (203)]. We investigated the effect of CQ (5 µM) on 100 key metabolite concentrations in HUH6 cell line, using a liquid chromatography-mass spectrophotometry based method. This profiling identified 12 significantly decreased metabolites and 4 significantly increase metabolites in CQ treated cells compared to the control (**Table 7**).

**Table 7. Statistically significantly altered metabolites after 96h CQ (5 µM) treatment.**

| Metabolite | FC | P-value |
|---|---|---|
| $NAD^+$ | 0.39903 | 0.0006958 |
| Myoinositol | 0.46644 | 0.0028352 |
| 4-Pyridoxic Acid | 3.1111 | 0.0049283 |
| Lysine | 3.043 | 0.0075209 |
| Aspartate | 0.25574 | 0.0087533 |
| Betaine | 0.095446 | 0.0096113 |
| Arginine | 2.5807 | 0.011984 |
| GABA | 0.10494 | 0.027384 |
| Creatine | 0.32802 | 0.027633 |
| Isovalerylcarnitine | 0.274 | 0.027858 |
| ADMA | 2.5424 | 0.028598 |
| Carnitine | 0.14461 | 0.029634 |
| Phosphoethanolamine | 0.12009 | 0.032194 |
| Hydroxyproline | 0.41124 | 0.040055 |
| Taurine | 0.37727 | 0.04041 |
| cAMP | 0.45375 | 0.041231 |

Metabolite enrichment analysis highlighted malate-aspartate shuttle to be most abundantly altered pathway (>12-fold increase; **Figure 24A**). Aspartate was also denoted to be significantly changed in single metabolite analysis; a 75 % reduction in aspartate concentration was observed in CQ treated vs. control cells (**Figure 24B**). Interestingly, aspartate supplementation was able to rescue HUH6 cells from CQ induced cell death (**Figure 24C**) suggesting that aspartate availability limits HB cell survival. A similar effect on aspartate availability was demonstrated in pancreatic cancer cells treated with CQ (110), suggesting that aspartate biosynthesis may be crucial target of this drug in cancer cells.

The most significantly altered single metabolite was nicotine adenine dinucleotide ($NAD^+$) which was reduced 60 % after CQ treatment compared to cells receiving control treatment (**Figure 24D**). Furthermore, a substantially higher proportion of the NAD pool was in the hydrogenated NADH form in CQ treated cells (**Figure 24E**), suggesting that CQ impacts the regulation of NAD redox balance. $NAD^+$ has an important role in variety of cellular processes such as DNA-damage response, biosynthesis, and energy metabolism [reviewed in (204)]. Altered $NAD^+$ synthesis has been studied as a vulnerability for cancer treatment (205,206).

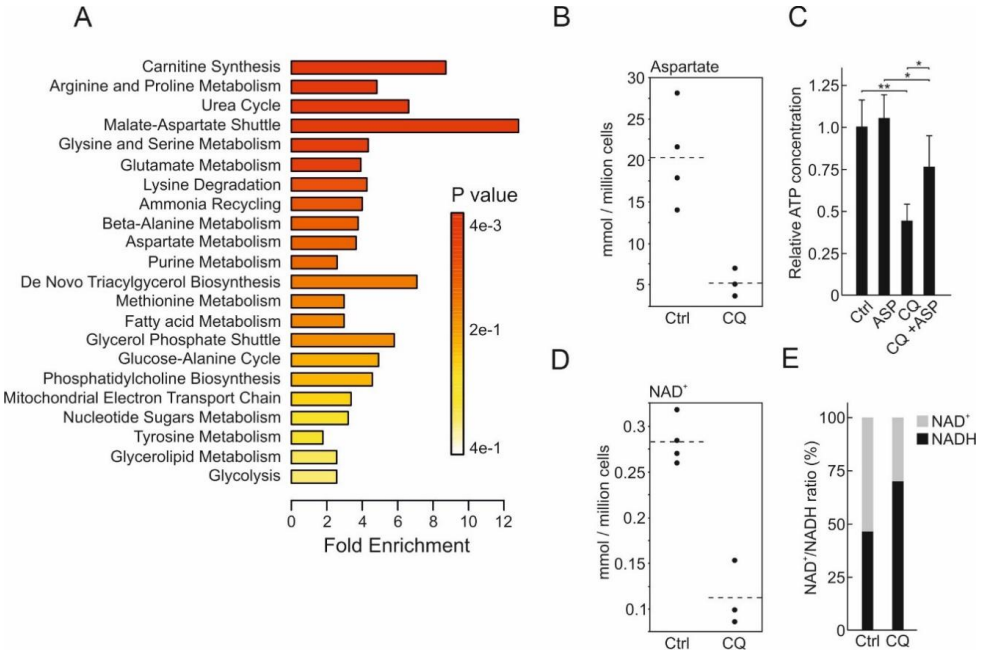


**Figure 24. Enriched metabolites in HUH6 cells treated with 5 µM of CQ.** *Metabolite enrichment analysis demonstrated significant over representation of malate-asparte shuttle related metabolism (A). Aspartate concentration decreased 75 % after CQ treatment (B). Aspartate supplementation rescued HUH6 cells from CQ triggered decrease in viability (C). Asparate did not show independent effect on viability (C). $NAD^+$ concentration decreased 60 % in CQ treated cells versus control treatment (D). CQ shifted $NAD^+$/NADH balance towards reduced form (E). Bar plots are presented as relative values of mean ± RSD *=p-value<0.05. **p-value<0.01. CQ=chloroquine. ASP=aspartate (10 mM).*

### 3.3 Cell death associated gene expression changes after chloroquine treatment

To elucidate molecular mechanisms by which CQ triggers cell death in HB cells, we performed Cell Death Pathway RT-qPCR array. This array detected 16/84 differentially expressed genes (**Table 8**) in HUH6 cells treated with 5 µM CQ for 96 h: 6 genes were associated with apoptosis (*CD40LG, CD40, TNF, TP53, IFNG*, and *ABL1*), 5 genes related to autophagy (*ESR1*, *IGF1*, *SQSTM1*, *BECN1*, and *CTSS*), and 5 classified as necroptotic (*PARP1, PARP2, FOXI1, TXNL4B*, and *DPYSL4*).

**Table 8. Altered death signaling associated genes after CQ treatment.**

| Gene symbol | CQ/CTRL ratio | p-value |
|---|---|---|
| *ABL1* | 0.717701297 | 0.012529 |
| *BECN1* | 0.653456319 | 0.043648 |
| *CD40* | 2.067471422 | 0.019648 |
| *CD40LG* | 2.19819468 | 0.013018 |
| *CTSS* | 1.933634249 | 0.01345 |
| *DPYSL4* | 1.466136062 | 0.031811 |
| *ESR1* | 1.600920652 | 0.041962 |
| *FOXI1* | 2.576141567 | 0.012603 |
| *IFNG* | 1.803772764 | 0.031009 |
| *IGF1* | 0.539850609 | 0.012628 |
| *PARP1* | 0.703267209 | 0.022517 |
| *PARP2* | 0.616548596 | 0.015909 |
| *SQSTM1* | 1.206510976 | 0.031734 |
| *TNF* | 2.348296095 | 0.002528 |
| *TP53* | 1.316000176 | 0.019288 |
| *TXNL4B* | 0.808867464 | 0.000391 |

### 3.4 CQ attenuates PARP expression in HB cells

Considering that we observed decreased $NAD^+$ concentrations in our metabolomic profiling and the fact that action of poly(ADP)-ribose polymerase (PARP) is dependent on $NAD^+$ availability (207), PARP was chosen for further analysis. PARP1 and PARP2 protein expression was evaluated in three HB cell lines treated with 5 μM of CQ utilizing western blotting. By this method, we observed statistically significantly reduced PARP1 expression in 2/3 cell lines (**Figure 25A**) whereas PARP2 expression decreased in one of studied models (**Figure 25B**). Furthermore, we performed immunofluorescence staining to validate localization of PARP1 in HUH6 cells. After 96 h CQ treatment, nuclear PARP1 expression decreases remarkably (**Figure 25C**). Taken together, $NAD^+$ depletion mediated PARP inhibition seems to be one of the mechanisms of action for CQ in cancer.

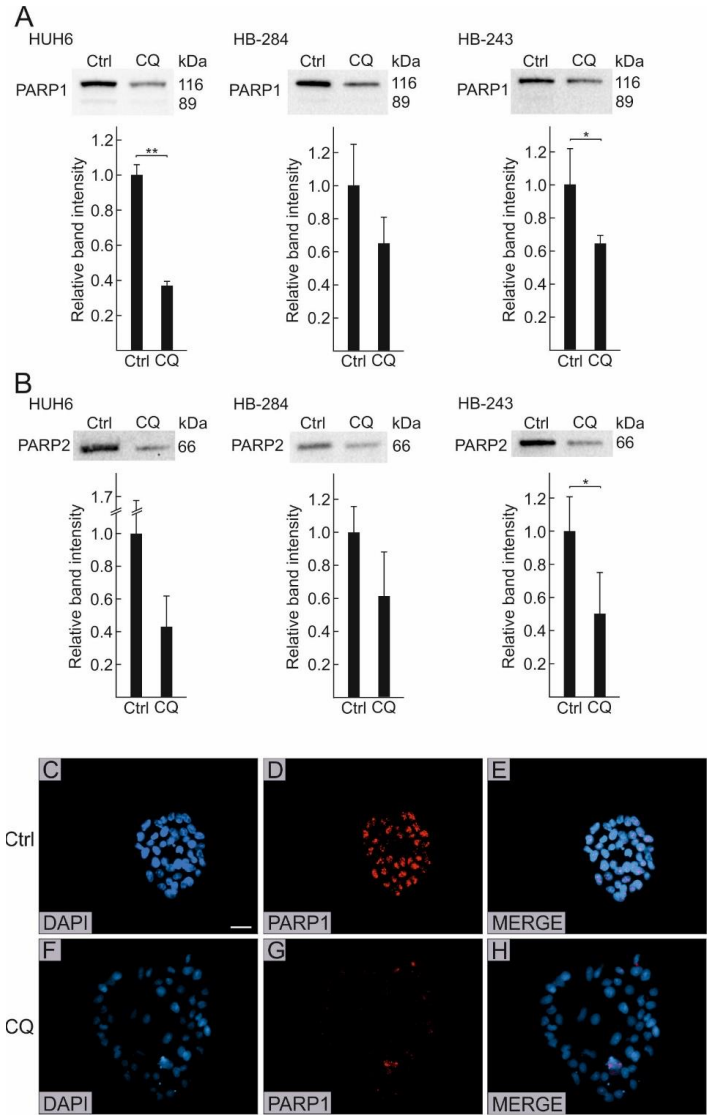


**Figure 25. PARP expression in HB cells after treatment with 5 µM CQ.** *Statistically significant decrease in PARP1 expression is evident in 2/3 HB cell lines (A). PARP2 expression is reduced significantly in 1/3 HB cell lines (B). Bar plots are represented as a mean of three experiment ±RSD. Band intensity is normalized to total protein expression of corresponding lane. PARP1 is expressed mainly in nuclei of HUH6 cells (C-E). Drastic decrease in PARP1 positive nuclei is observed after CQ treatment (F-H).*

PARPs are involved in various processes in cancer cells including epigenetic modification, DNA-damage response, and signal transduction [reviewed in (208)]. Small molecule PARP inhibitors have been utilized in treatment of several cancers including ovarian cancer and breast cancer (209,210). Interestingly, abundant activation

of PARP1 has been reported in HB cells and it is associated with modification of aberrantly expressed tumor suppressor genes (211). Moreover, it has been suggested that CQ may potentiate the effect of PARP inhibitors; for example, this has been demonstrated in HCC treated with nirabarib and CQ (212). In sum, abundant PARP expression has been shown to be important for hepatocellular malignant behavior and CQ attenuates PARP expression proposing that CQ could be beneficial in management of aggressive HB either as a monotherapy or combined with other agents.

### 3.5 Summary of the findings related to CQ treatment in HB

We observed markedly decreased cell viability and increased apoptosis in seven HB spheroid model treated with CQ (1 μM, 5 μM, or 10 μM). These effects were both time- and dose-dependent in most of the models. Similarly, cell viability was decreased in 2D cell cultures treated with fixed doses of CQ. Metabolomic profiling demonstrated altered aspartate and $NAD^+$ metabolism after CQ treatment. Aspartate supplementation was able to rescue HB cells from CQ induced cell death suggesting that cancer cells sensitive to aspartate depletion are potential targets of CQ treatment. We also observed reduced PARP1/2 mRNA and protein expression in HB cells treated with CQ. As PARP function is $NAD^+$-dependent, metabolic changes caused by CQ administration may inhibit PARPs, indicating that CQ also has potential in treatment of cancers sensitive to PARP inhibitors. A schematic view of the proposed mechanisms of action is shown in **Figure 26**.

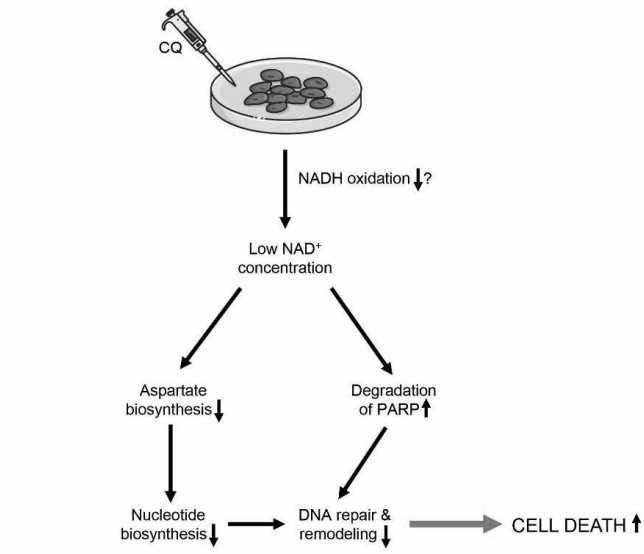


**Figure 26. Proposed mechanisms of CQ treatment in HB cells.**

# CONCLUSIONS AND FUTURE DIRECTIONS

This study elucidated molecular mechanisms involved in HB pathogenesis including aberrant gene expression and metabolic vulnerabilities (summarized in **Figure 27**). We identified potential targets for novel therapeutic approaches in HB and introduced new mechanism of actions for CQ in cancer cells.

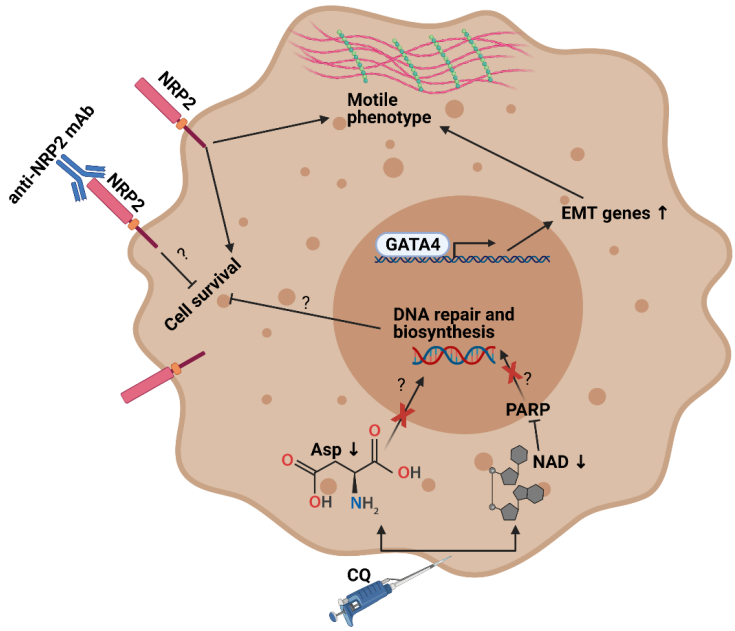


**Figure 27. Summary of the observations described in this thesis.** *High GATA4 expression was detected in HBs and was associated with upregulation of EMT-related genes and increased motility (I). Abundant NRP2 expression was noted in HB patient samples and cell lines (II) and was linked to cell survival and migration which may be attenuated with anti-NRP mAb. CQ decreased aspartate (Asp) and $NAD^+$ concentration in HB cells (III). Moreover, decreased PARP expression was observed after CQ administration. We suggest that these mechanisms reduce nucleotide biosynthesis and DNA-damage repair response leading to cell death. Figure was created with BioRender.com.*

Aim-by-aim conclusions and future directions:

1. Transcription factor GATA4 is crucial for the early stages of normal liver development [reviewed in (21)]. Our study demonstrated high GATA4 in majority of HB patient samples and PDX-derived cell lines, underscoring the notion that HB cells arise from the early hepatic progenitor cells. *In vitro*, *GATA4* silencing changed the expression of EMT-associated genes suggesting that GATA4 maintains similar

processes in HB than its physiological tasks are during the development. Furthermore, silenced *GATA4* expression led to altereted cell junction dynamics and cytoskeleton structure in HB cells linking GATA4 with the mesenchymal phenotype in HB.

In future studies, the findings described herein should be assessed in animal models or organoids to confirm the role of GATA4 in HB pathogenesis.

2. NRPs are multifunctional non-tyrosine kinase receptors involved in pathogenesis of multiple cancers [reviewed in (213)]. Monoclonal antibodies targeting NRP2 have been developed as potential therapies (192). We observed that NRP1 and NRP2 are highly expressed in HBs whereas normal hepatocytes do not display these markers, indicating that NRP expression is a tumor-specific feature. *NRP2* silencing decreased cell survival and motility suggesting that therapeutic interventions targeting NRP2 may have potential in the management of aggressive HB.

In our study, the number of patient samples was limited, and our observations need to be confirmed in a larger sample set. Moreover, the correlation between NRP expression and clinical variables should be evaluated to assess the potential of NRPs as prognostic biomarkers in HB. Additionally, the efficacy of anti-NRP2 monoclonal antibodies should be investigated in future *in vitro* and *in vivo* studies to assess their potential in HB treatment.

3. Several clinical trials studying the potential of CQ in the treatment of advanced cancer are ongoing or completed [reviewed in (214)]. We noted a time- and dose-dependent effect of CQ on cell viability and apoptosis rate in our 3D HB cell models suggesting that CQ has anti-tumorigenic potential in HB. Furthermore, CQ treatment led to a reduction of aspartate concentration, and CQ triggered cell death was rescued with aspartate supplementation suggesting that HB cells are dependent on aspartate availability. $NAD^+$/NADH balance shifted towards NADH after CQ treatment. We propose that this reduction in $NAD^+$ availability impairs PARP expression and function as we observed decrease in PARP1 and PARP2 expression at mRNA and protein level 96 h post-treatment.

As a next step, CQ efficacy should be studied in mice models as a monotherapy or combined with the traditional HB chemotherapeutics cisplatin and doxorubicin. In the future, these results may be translated to clinic and CQ could be included into HB trials.

## Acknowledgements

This thesis project was carried out in the Pediatric Research Center of Children's Hospital, Biomedicum Helsinki, University of Helsinki, Finland. I wish to acknowledge those who provided me with excellent research facilities and outstanding scientific training: Docent *Jari Petäjä*, the Director of the Children's Hospital, Professor *Kaija-Leena Kolho*, the Chairman of Children's Hospital, Professor *Markku Heikinheimo*, the previous Chairman of Children's Hospital, Professor *Kim Vettenranta*, the Head of Pediatric Graduate School, and Professor *Taneli Raivio*, the Director of Pediatric Research Center and the Chairman of Doctoral Programme in Clinical Research.

I express my gratitude for the salary-funded doctoral candidate position in the Doctoral Programme in Clinical Research at University of Helsinki enabling me to focus on full-time research. These thesis projects received financial support from the Aamu Pediatric Cancer Foundation, Academy of Finland, Cancer Foundation Finland, Finnish Pediatric Research Foundation, Finska Läkaresällskapet, Helsinki University Central Hospital Research Grants, Päivikki and Sakari Sohlberg Foundation, and Sigrid Jusélius Foundation.

I am grateful to my official reviewers Professors *Anna-Liisa Levonen* and *Risto Kerkelä* for their time, expertise, and valuable suggestions to improve this thesis. My thesis committee members Docent *Jussi Merenmies* and Professor *Juha Tapanainen* are thanked for their support and advices during this project.

I owe my most sincere gratitude to my supervisors Professor *Markku Heikinheimo* and Docent *Marjut Pihlajoki*. *Markku*, I admire your wide scientific knowledge and expertise as well as your relaxed attitude towards life. You have an amazing ability to recognize strengths of young scientists and nourish those skills. I am grateful that you have been supporting my growth to be an independent scientist in the future. *Marjut*, you have been present almost on every single day of my PhD journey and I am most grateful for that. I express thousands of thanks to you for reassuring me when there have been days when everything has failed and your willingness to help with experiments when ever it has been needed. Your problem-solving skills are stunning, and I revere how kind you are to everyone around you no matter how busy you are.

My warmest thanks to numerous outstanding and talented collaborators and co-authors without whom these projects would have never been possible. I thank Doctor *Tea Soini* for introducing the world of hepatoblastoma research to me and inspiring me to continue with this topic. I am grateful to Professor *David B. Wilson* for pleasant collaboration and constructive suggestions to improve projects included in this thesis. *Dave* is also thanked for revising the language of this thesis. I express my thanks to Doctor *Stefano Cairo* for bringing valuable new resources and amazing amount of expertise in hepatoblastoma research to these projects. Professor *Mikko Pakarinen* and Doctor *Antti Kyrönlahti* have been highly valued links to hepatoblastoma patients in Children's Hospital and I thank them for their help and advices. Docent *Jouko Lohi*, Doctor *Noora Andersson*, Doctor

*Jean-Gabriel Judde*, *Emmi Liljeström*, and *Ruth Nousiainen* are thanked for their essential contribution to studies in this thesis.

I have felt often that the lab has been literally my second home. Considering that fact, it has been great privilege to be surrounded by skilled and friendly colleagues and co-workers. *Noora Andersson*, *Saara Bryk*, *Nimish Godbole*, *Ulla-Maija Haltia*, *Tuike Helmiö*, *Otto Helve*, *Pyry Jaakkola*, *Anu Kaskinen*, *Antti Kyrönlahti*, *Emmi Liljeström*, *Sari Linden*, *Ruth Nousiainen*, *Iiris Nyholm*, and *Tea Soini* are warmly thanked for all the help with experiments as well as creating working environment full of joy and laughs. Moreover, I want to thank you all for your friendship, it has been great pleasure to get to know you all. A special thanks to *Iiris*, my fellow PhD candidate, for inspiring conversations about both science and subjects beyond that. Those hours spent together in the lab after 4 pm have brought me many new perspectives and above all, it has been fun.

I have been extremely lucky to find so many amazing friends. *Kaisa*, thank you for dragging me to the far-away countries and forests near-by to keep balance in my life when this thesis project tried to conquer all parts of it. Spending time with you has usually guarantee that something crazy will happen and it has brought so much happiness into my life. *Noora*, we share over two decades of history and passion for cats, science, and cakes. I want to thank you for your great advices in life and science and all the endless and almost daily conversations about academic life as well as everything between heaven and earth. *Noora* is also thanked for designing the cover for this book. Thank you *Anni* and *Paula* for all your support, long conversations about everything, and bringing a great amount of joy to my life when it has been needed. *Emma*, thank you for the peer-support in journey to the medical sciences and distractions in forms of coffee and brunches. *Henkka*, thank you for sending me cat videos when stress was taking over and moreover, I want to acknowledge you for introducing Python to me. *Taru*, our kickboxing exercises in the early mornings gave a great start for working days and I am thankful that we used to have that routine.

My heartfelt thanks to my dear parents, *Jaana* and *Esa*, who has always believed in me and encouraged me to pursue my dreams. Thank you for making me who I am today and supporting me in everything. Without your love and encouragement, I wouldn't be writing this today. I thank *Jani* for all the valuable moments shared together. I want to thank also my grandmother *Eila* and all the other *Haiko* and *Eloranta* family members who have been supporting my journey. I am grateful to my in-laws in *Vainio* family for all the great moments spent together. These family gatherings have offered needed break from my research work.

Finally, I want to thank my beloved *Joonas* for all love and care. You make me believe that anything is possible, and I am most grateful for having you on my side. I love you and our furry babies Fiona and Ninja more than anything.

**Helsinki, May 2021**

*Katja Eloranta*

# References


1. Kung JWC, Currie IS, Forbes SJ, Ross JA. Liver development, regeneration, and carcinogenesis. Hay DC, editor. J Biomed Biotechnol. 2010;2010:984248.

2. Lee CS, Friedman JR, Fulmer JT, Kaestner KH. The initiation of liver development is dependent on Foxa transcription factors. Nature. 2005;435(7044):944–7.

3. Zhao R, Watt AJ, Li J, Luebke-Wheeler J, Morrisey EE, Duncan SA. GATA6 Is Essential for Embryonic Development of the Liver but Dispensable for Early Heart Formation. Mol Cell Biol. 2005;25(7):2622–31.

4. Rossi JM, Dunn NR, Hogan BLM, Zaret KS. Distinct mesodermal signals, including BMPs from the septum, transversum mesenchyme, are required in combination for hepatogenesis from the endoderm. Genes Dev. 2001;15(15):1998–2009.

5. Jung J, Zheng M, Goldfarb M, Zaret KS. Initiation of mammalian liver development from endoderm by fibroblast growth factors. Science (80- ). 1999;284(5422):1998–2003.

6. Tanimizu N, Miyajima A. Molecular Mechanism of Liver Development and Regeneration. Vol. 259, International Review of Cytology. 2007. p. 1–48.

7. Cocjin J, Rosenthal P, Buslon V, Luk L, Barajas L, Geller SA, Ruebner B, French S. Bile ductule formation in fetal, neonatal, and infant livers compared with extrahepatic biliary atresia. Hepatology. 1996;24(3):568–74.

8. Terada T, Nakanuma Y. Development of human peribiliary capillary plexus: A lectin-histochemical and immunohistochemical study. Hepatology. 1993;18(3):529–36.

9. Watt AJ, Garrison WD, Duncan SA. HNF4: A central regulator of hepatocyte differentiation and function. Vol. 37, Hepatology. 2003. p. 1249–53.

10. Clotman F, Lannoy VJ, Reber M, Cereghini S, Cassiman D, Jacquemin P, Roskams T, Rousseau GG, Lemaigre FP. The onecut transcription factor HNF6 is required for normal development of the biliary tract. Vol. 129, Development. 2002. p. 1819–28.

11. Poncy A, Antoniou A, Cordi S, Pierreux CE, Jacquemin P, Lemaigre FP. Transcription factors SOX4 and SOX9 cooperatively control development of bile ducts. Dev Biol. 2015;404(2):136–48.

12. Sibulesky L. Normal liver anatomy. Vol. 2, Clinical Liver Disease. 2013.

13. Pryce JW, Bamber AR, Ashworth MT, Kiho L, Malone M, Sebire NJ. Reference ranges for organ weights of infants at autopsy: Results of >1,000 consecutive cases from a single centre. BMC Clin Pathol. 2014;14(1):1–12.

14. Mitra V, Metcalf J. Functional anatomy and blood supply of the liver. Vol. 13, Anaesthesia and Intensive Care Medicine. 2012. p. 52–3.

15. Strazzabosco M, Fabris L. Functional anatomy of normal bile ducts. Anat Rec. 2008;291(6):653–60.

16. Corless JK, Middleton HM. Normal Liver Function: A Basis for Understanding Hepatic Disease. Arch Intern Med. 1983;143(12):2291–4.

17. Gebhardt R. Metabolic zonation of the liver: Regulation and implications for liver function. Vol. 53, Pharmacology and Therapeutics. 1992. p. 275–354.

18. Erker L, Grompe M. Signaling networks in hepatic oval cell activation. Vol. 1, Stem Cell Research. 2008. p. 90–102.

19. Aizarani N, Saviano A, Sagar, Mailly L, Durand S, Herman JS, Pessaux P, Baumert TF, Grün D. A human liver cell atlas reveals heterogeneity and epithelial progenitors. Nature. 2019;572(7768):199–204.

20. Zhao J, Zhang S, Liu Y, He X, Qu M, Xu G, Wang H, Huang M, Pan J, Liu Z, Li Z, Liu L, Zhang Z. Single-cell RNA sequencing reveals the heterogeneity of liver-resident immune cells in human. Cell Discov. 2020;6(1).

21. Si-Tayeb K, Lemaigre FP, Duncan SA. Organogenesis and Development of the Liver. Vol. 18, Developmental Cell. 2010. p. 175–89.

22. Ng K, Mogul DB. Pediatric Liver Tumors. Vol. 22, Clinics in Liver Disease. 2018. p. 753–72.

23. Feng J, Polychronidis G, Heger U, Frongia G, Mehrabi A, Hoffmann K. Incidence trends and survival prediction of hepatoblastoma in children: A population-based study. Cancer Commun. 2019;39(1).

24. Tiusanen T, Hukkinen M, Leskinen O, Soini T, Kanerva JA, Jahnukainen T, Mäkisalo H, Heikinheimo M, Pakarinen MP. Incidence and long-term outcomes of surgically treated childhood hepatic malignancies in Finland. Acta Paediatr Int J Paediatr. 2020;109(2):404–14.

25. Darbari A, Sabin KM, Shapiro CN, Schwarz KB. Epidemiology of primary hepatic malignancies in U.S. children. Hepatology. 2003;38(3):560–6.

26. Litten JB, Tomlinson GE. Liver tumors in children. Oncologist. 2008;13(7):812–20.

27. Prokurat A, Kluge P, Kociesza A, Perek D, Kappeler A, Zimmermann A. Transitional liver cell tumors (TLCT) in older children and adolescents: A novel group of aggressive hepatic tumors expressing beta-catenin. In: Medical and Pediatric Oncology. 2002. p. 510–8.

28. Spector LG, Birch J. The epidemiology of hepatoblastoma. Vol. 59, Pediatric Blood and Cancer. 2012. p. 776–9.

29. De Fine Licht S, Schmidt LS, Rod NH, Schmiegelow K, Lähteenmäki PM, Kogner P, Träger C, Stokland T, Schüz J. Hepatoblastoma in the Nordic countries. Int J Cancer. 2012;131(4).

30. Jung SE, Kim KH, Kim MY, Kim DY, Lee SC, Park KW, Kim WK. Clinical characteristics and prognosis of patients with hepatoblastoma. World J Surg. 2001;25(2):126–30.

31. Sotelo-Avila C, Gonzalez-Crussi F, Fowler JW. Complete and incomplete forms of Beckwith-Wiedemann syndrome: Their oncogenic potential. J Pediatr. 1980;96(1):47–50.

32. Mussa A, Russo S, Larizza L, Riccio A, Ferrero GB. (Epi)genotype–phenotype correlations in Beckwith–Wiedemann syndrome: a paradigm for genomic medicine. Clin Genet. 2016 Apr 1;89(4):403–15.

33. Kato M, Takita J, Takahashi K, Mimaki M, Chen Y, Koh K, Ida K, Oka A, Mizuguchi M, Ogawa S, Igarashi T. Hepatoblastoma in a patient with Sotos syndrome. J Pediatr. 2009;155(6):937–9.

34. Ueno Y, Katayama S, Goto T, Nakahara Y, Hitomi K. A Girl With Sotos Syndrome and Hepatoblastoma. J Japanese Soc Pediatr Surg. 2020;56(6):939–43.

35. Hughes LJ, Michels V V. Risk of hepatoblastoma in familial adenomatous polyposis. Am J Med Genet. 1992;43(6):1023–5.

36. Tan ZH, Lai A, Chen CK, Chang KTE, Tan AM. Association of trisomy 18 with hepatoblastoma and its implications. Eur J Pediatr. 2014;173(12):1595–8.

37. Heck JE, Meyers TJ, Lombardi C, Park AS, Cockburn M, Reynolds P, Ritz B. Case-control study of birth characteristics and the risk of hepatoblastoma. Cancer Epidemiol. 2013;37(4):390–5.

38. Tanimura M, Matsui I, Abe J, Ikeda H, Kobayashi N, Ohira M, Yokoyama M, Kaneko M. Increased Risk of Hepatoblastoma among Immature Children with a Lower Birth Weight. Cancer Res. 1998 Jul 15;58(14):3032 LP – 3035.

39. Spector LG, Johnson KJ, Soler JT, Puumala SE. Perinatal risk factors for hepatoblastoma. Br J Cancer. 2008;98(9):1570–3.

40. Feusner J, Plaschkes J. Hepatoblastoma and low birth weight: A trend or chance observation? Med Pediatr Oncol. 2002;39(5):508–9.

41. McLaughlin CC, Baptiste MS, Schymura MJ, Nasca PC, Zdeb MS. Maternal and infant birth characteristics and hepatoblastoma. Am J Epidemiol. 2006;163(9):818–28.

42. Musselman JRB, Georgieff MK, Ross JA, Tomlinson GE, Feusner J, Krailo M, Spector LG. Maternal pregnancy events and exposures and risk of hepatoblastoma: A Children's Oncology Group (COG) study. Cancer Epidemiol. 2013;37(3):318–20.

43. De Ioris M, Brugieres L, Zimmermann A, Keeling J, Brock P, Maibach R, Pritchard J, Shafford L, Zsiros J, Czaudzerna P, Perilongo G. Hepatoblastoma with a low serum alpha-fetoprotein level at diagnosis: The SIOPEL group experience. Eur J Cancer. 2008;44(4):545–50.

44. Liu W, Chen S, Liu B. Diagnostic and prognostic values of serum exosomal microRNA-21 in children with hepatoblastoma: a Chinese population-based study. Pediatr Surg Int. 2016;32(11):1059–65.

45. Zhou S, O'Gorman MRG, Yang F, Andresen K, Wang L. Glypican 3 as a Serum Marker for Hepatoblastoma. Sci Rep. 2017;7.

46. Molina L, Bell D, Tao J, Preziosi M, Pradhan-Sundd T, Singh S, Poddar M, Luo J, Ranganathan S, Chikina M, Monga SP. Hepatocyte-Derived Lipocalin 2 Is a Potential Serum Biomarker Reflecting Tumor Burden in Hepatoblastoma. Am J Pathol. 2018;188(8):1895–909.

47. Falix FA, Aronson DC, Lamers WH, Hiralall JK, Seppen J. DLK1, a serum marker for hepatoblastoma in young infants. Pediatr Blood Cancer. 2012;59(4):743–5.

48. Kremer N, Walther AE, Tiao GM. Management of hepatoblastoma: An update. Vol. 26, Current Opinion in Pediatrics. 2014. p. 362–9.

49. Weinberg AG, Finegold MJ. Primary hepatic tumors of childhood. Hum Pathol. 1983;14(6):512–37.

50. Kiruthiga KG, Ramakrishna B, Saha S, Sen S. Histological and immunohistochemical study of hepatoblastoma: Correlation with tumour behaviour and survival. J Gastrointest Oncol. 2018;9(2):326–37.

51. Fabre M, Yilmaz F, Buendia MA. Hepatic tumors in childhood: Experience on 245 tumors and review of literature. Vol. 24, Annales de Pathologie. 2004. p. 536–55.

52. Shabanov MA, Liubimova OE, Raĭkhlin NT, Adne ZZ. Hepatoblastoma cells producing alpha-fetoprotein: morphometric, immunohistochemical and electron microscopic studies.

Arkh Patol. 1987;49(12):9–16.

53. Koh KN, Park M, Kim BE, Bae KW, Kim KM, Im HJ, Seo JJ. Prognostic implications of serum alpha-fetoprotein response during treatment of hepatoblastoma. Pediatr Blood Cancer. 2011;57(4):554–60.

54. Abenoza P, Manivel JC, Wick MR, Hagen K, Dehner LP. Hepatoblastoma: An immunohistochemical and ultrastructural study. Hum Pathol. 1987;18(10):1025–35.

55. Ranganathan S, Lopez-Terrada D, Alaggio R. Hepatoblastoma and Pediatric Hepatocellular Carcinoma: An Update. Vol. 23, Pediatric and Developmental Pathology. 2020. p. 79–95.

56. Aguiar TFM, Carneiro TN, da Costa CML, Rosenberg C, da Cunha IW, Krepischi ACV. The genetic and epigenetic landscapes of hepatoblastomas. Appl Cancer Res. 2017;37(1).

57. Tomlinson GE, Douglass EC, Pollock BH, Finegold MJ, Schneider NR. Cytogenetic evaluation of a large series of hepatoblastomas: Numerical abnormalities with recurring aberrations involving 1q12-q21. Genes Chromosom Cancer. 2005;44(2):177–84.

58. Schneider NR, Cooley LD, Finegold MJ, Douglass EC, Tomlinson GE. The first recurring chromosome translocation in hepatoblastoma: Der(4)t(1;4)(q12;q34). Genes Chromosom Cancer. 1997;19(4):291–4.

59. Cairo S, Armengol C, De Reyniès A, Wei Y, Thomas E, Renard CA, Goga A, Balakrishnan A, Semeraro M, Gresh L, Pontoglio M, Strick-Marchand H, Levillayer F, Nouet Y, Rickman D, Gauthier F, Branchereau S, Brugières L, Laithier V, Bouvier R, Boman F, Basso G, Michiels JF, Hofman P, Arbez-Gindre F, Jouan H, Rousselet-Chapeau MC, Berrebi D, Marcellin L, Plenat F, Zachar D, Joubert M, Selves J, Pasquier D, Bioulac-Sage P, Grotzer M, Childs M, Fabre M, Buendia MA. Hepatic Stem-like Phenotype and Interplay of Wnt/β-Catenin and Myc Signaling in Aggressive Childhood Liver Cancer. Cancer Cell. 2008;14(6):471–84.

60. Zhang Y, Wang X. Targeting the Wnt/β-catenin signaling pathway in cancer. J Hematol Oncol. 2020;13(1):165.

61. Udatsu Y, Kusafuka T, Kuroda S, Miao J, Okada A. High frequency of β-catenin mutations in hepatoblastoma. Pediatr Surg Int. 2001;17(7):508–12.

62. Koch A, Denkhaus D, Albrecht S, Leuschner I, Von Schweinitz D, Pietsch T. Childhood hepatoblastomas frequently carry a mutated degradation targeting box of the β-catenin gene. Cancer Res. 1999;59(2):269–73.

63. López-Terrada D, Gunaratne PH, Adesina AM, Pulliam J, Hoang DM, Nguyen Y, Mistretta TA, Margolin J, Finegold MJ. Histologic subtypes of hepatoblastoma are characterized by differential canonical Wnt and Notch pathway activation in DLK+ precursors. Hum Pathol. 2009;40(6):783–94.

64. Pei Y, Kano J, Iijima T, Morishita Y, Inadome Y, Noguchi M. Overexpression of Dickkopf 3 in hepatoblastomas and hepatocellular carcinomas. Virchows Arch. 2009;454(6):639–46.

65. Cairo S, Armengol C, Buendia MA. Activation of Wnt and Myc signaling in hepatoblastoma. Front Biosci - Elit. 2012;4 E(1):480–6.

66. Purcell R, Childs M, Maibach R, Miles C, Turner C, Zimmermann A, Sullivan M. HGF/c-Met related activation of β-catenin in hepatoblastoma. J Exp Clin Cancer Res. 2011;30(1):96.

67. Eichenmüller M, Gruner I, Hagl B, Häberle B, Müller-Höcker J, von Schweinitz D, Kappler R. Blocking the hedgehog pathway inhibits hepatoblastoma growth. Hepatology.

2009;49(2):482–90.

68. Gray SG, Eriksson T, Ekström C, Holm S, Von Schweinitz D, Kogner P, Sandstedt B, Pietsch T, Ekström TJ. Altered expression of members of the IGF-axis in hepatoblastomas. Br J Cancer. 2000;82(9):1561–7.

69. Tao J, Calvisi DF, Ranganathan S, Cigliano A, Zhou L, Singh S, Jiang L, Fan B, Terracciano L, Armeanu-Ebinger S, Ribback S, Dombrowski F, Evert M, Chen X, Monga SPS. Activation of β-catenin and Yap1 in human hepatoblastoma and induction of hepatocarcinogenesis in mice. Gastroenterology. 2014;147(3):690–701.

70. Cairo S, Armengol C, Maibach R, Häberle B, Becker K, Carrillo-Reixach J, Guettier C, Vokuhl C, Schmid I, Buendia MA, Branchereau S, von Schweinitz D, Kappler R. A combined clinical and biological risk classification improves prediction of outcome in hepatoblastoma patients. Eur J Cancer. 2020;141:30–9.

71. Carrillo-Reixach J, Torrens L, Simon-Coma M, Royo L, Domingo-Sàbat M, Abril-Fornaguera J, Akers N, Sala M, Armengol C, et al. Epigenetic footprint enables molecular risk stratification of hepatoblastoma with clinical implications. J Hepatol. 2020;73(2):328–41.

72. Towbin AJ, Meyers RL, Woodley H, Miyazaki O, Weldon CB, Morland B, Hiyama E, Czauderna P, Roebuck DJ, Tiao GM. 2017 PRETEXT: radiologic staging system for primary hepatic malignancies of childhood revised for the Paediatric Hepatic International Tumour Trial (PHITT). Pediatric Radiology. 2018.

73. Meyers RL, Maibach R, Hiyama E, Häberle B, Krailo M, Rangaswami A, Aronson DC, Malogolowkin MH, Perilongo G, von Schweinitz D, Ansari M, Lopez-Terrada D, Tanaka Y, Alaggio R, Leuschner I, Hishiki T, Schmid I, Watanabe K, Yoshimura K, Feng Y, Rinaldi E, Saraceno D, Derosa M, Czauderna P. Risk-stratified staging in paediatric hepatoblastoma: a unified analysis from the Children's Hepatic tumors International Collaboration. Lancet Oncol. 2017;18(1):122–31.

74. Malogolowkin MH, Katzenstein HM, Meyers RL, Krailo MD, Rowland JM, Haas J, Finegold MJ. Complete surgical resection is curative for children with hepatoblastoma with pure fetal histology: A report from the Children's Oncology Group. J Clin Oncol. 2011;29(24):3301–6.

75. Haas JE, Feusner JH, Finegold MJ. Small cell undifferentiated histology in hepatoblastoma may be unfavorable. Cancer. 2001;92(12):3130–4.

76. Perilongo G, Maibach R, Shafford E, Brugieres L, Brock P, Morland B, de Camargo B, Zsiros J, Roebuck D, Zimmermann A, Aronson D, Childs M, Widing E, Laithier V, Plaschkes J, Pritchard J, Scopinaro M, MacKinlay G, Czauderna P. Cisplatin versus Cisplatin plus Doxorubicin for Standard-Risk Hepatoblastoma. N Engl J Med. 2009 Oct 22;361(17):1662–70.

77. Zsíros J, Maibach R, Shafford E, Brugieres L, Brock P, Czauderna P, Roebuck D, Childs M, Zimmermann A, Laithier V, Otte JB, De Camargo B, MacKinlay G, Scopinaro M, Aronson D, Plaschkes J, Perilongo G. Successful treatment of childhood high-risk hepatoblastoma with dose-intensive multiagent chemotherapy and surgery: Final results of the SIOPEL-3HR study. J Clin Oncol. 2010;28(15):2584–90.

78. Pritchard J, Brown J, Shafford E, Perilongo G, Brock P, Dicks-Mireaux C, Keeling J, Phillips A, Vos A, Plaschkes J. Cisplatin, doxorubicin, and delayed surgery for childhood hepatoblastoma: A successful approach - Results of the first prospective study of the International Society of Pediatric Oncology. J Clin Oncol. 2000;18(22):3819–28.

79. Guo H-F, Vander Kooi CW. Neuropilin Functions as an Essential Cell Surface Receptor. J Biol Chem. 2015/10/08. 2015 Dec 4;290(49):29120–6.

80. Wild JRL, Staton CA, Chapple K, Corfe BM. Neuropilins: expression and roles in the epithelium. Int J Exp Pathol. 2012 Apr 1;93(2):81–103.

81. Rossignol M, Gagnon ML, Klagsbrun M. Genomic organization of human neuropilin-1 and neuropilin-2 genes: identification and distribution of splice variants and soluble isoforms. Genomics. 2000;70(2):211–22.

82. Chen H, Chédotal A, He Z, Goodman CS, Tessier-Lavigne M. Neuropilin-2, a Novel Member of the Neuropilin Family, Is a High Affinity Receptor for the Semaphorins Sema E and Sema IV but Not Sema III. Neuron. 1997;19(3):547–59.

83. Gagnon ML, Bielenberg DR, Gechtman Z, Miao HQ, Takashima S, Soker S, Klagsbrun M. Identification of a natural soluble neuropilin-1 that binds vascular endothelial growth factor: In vivo expression and antitumor activity. Proc Natl Acad Sci U S A. 2000 Mar 14;97(6):2573–8.

84. Cackowski FC, Xu L, Hu B, Cheng S-Y. Identification of two novel alternatively spliced Neuropilin-1 isoforms. Genomics. 2004;84(1):82–94.

85. Parker MW, Linkugel AD, Goel HL, Wu T, Mercurio AM, Vander Kooi CW. Structural Basis for VEGF-C Binding to Neuropilin-2 and Sequestration by a Soluble Splice Form. Structure. 2015;23(4):677–87.

86. Yuan L, Moyon D, Pardanaud L, Bréant C, Karkkainen MJ, Alitalo K, Eichmann A. Abnormal lymphatic vessel development in neuropilin 2 mutant mice. Development. 2002;129(20):4797–806.

87. Takashima S, Kitakaze M, Asakura M, Asanuma H, Sanada S, Tashiro F, Niwa H, Miyazaki J, Hirota S, Kitamura Y, Kitsukawa T, Fujisawa H, Klagsbrun M, Hori M. Targeting of both mouse neuropilin-1 and neuropilin-2 genes severely impairs developmental yolk sac and embryonic angiogenesis. Proc Natl Acad Sci. 2002 Mar 19;99(6):3657 LP – 3662.

88. Hasan NM, Kendrick MA, Druckenbrod NR, Huelsmeyer MK, Warner TF, MacDonald MJ. Genetic association of the neuropilin-1 gene with type 1 diabetes in children: Neuropilin-1 expression in pancreatic islets. Diabetes Res Clin Pract. 2010;87(3):e29–32.

89. Le A, Zielinski R, He C, Crow MT, Biswal S, Tuder RM, Becker PM. Pulmonary Epithelial Neuropilin-1 Deletion Enhances Development of Cigarette Smoke–induced Emphysema. Am J Respir Crit Care Med. 2009;180(5):396–406.

90. Takamatsu H, Okuno T, Kumanogoh A. Regulation of immune cell responses by semaphorins and their receptors. Cell Mol Immunol. 2010;7(2):83–8.

91. Cao S, Yaqoob U, Das A, Shergill U, Jagavelu K, Huebert RC, Routray C, Abdelmoneim S, Vasdev M, Leof E. Neuropilin-1 promotes cirrhosis of the rodent and human liver by enhancing PDGF/TGF-β signaling in hepatic stellate cells. J Clin Invest. 2010;120(7):2379–94.

92. Fukahi K, Fukasawa M, Neufeld G, Itakura J, Korc M. Aberrant Expression of Neuropilin-1 and -2 in Human Pancreatic Cancer Cells. Clin Cancer Res. 2004;10(2):581–90.

93. Kawakami T, Tokunaga T, Hatanaka H, Kijima H, Yamazaki H, Abe Y, Osamura Y, Inoue H, Ueyama Y, Nakamura M. Neuropilin 1 and neuropilin 2 co-expression is significantly correlated with increased vascularity and poor prognosis in nonsmall cell lung carcinoma. Cancer. 2002;95(10):2196–201.

94. Baba T, Kariya M, Higuchi T, Mandai M, Matsumura N, Kondoh E, Miyanishi M, Fukuhara K, Takakura K, Fujii S. Neuropilin-1 promotes unlimited growth of ovarian cancer by evading contact inhibition. Gynecol Oncol. 2007;105(3):703–11.

95. Hu B, Guo P, Bar-Joseph I, Imanishi Y, Jarzynka MJ, Bogler O, Mikkelsen T, Hirose T, Nishikawa R, Cheng SY. Neuropilin-1 promotes human glioma progression through potentiating the activity of the HGF/SF autocrine pathway. Oncogene. 2007;26(38):5577–86.

96. Parikh AA, Fan F, Liu WB, Ahmad SA, Stoeltzing O, Reinmuth N, Bielenberg D, Bucana CD, Klagsbrun M, Ellis LM. Neuropilin-1 in Human Colon Cancer: Expression, Regulation, and Role in Induction of Angiogenesis. Am J Pathol. 2004;164(6):2139–51.

97. Fakhari M, Pullirsch D, Abraham D, Paya K, Hofbauer R, Holzfeind P, Hofmann M, Aharinejad S. Selective upregulation of vascular endothelial growth factor receptors neuropilin-1 and -2 in human neuroblastoma. Cancer. 2002 Jan 1;94(1):258–63.

98. Dong X, Guo W, Zhang S, Wu T, Sun Z, Yan S, Zheng S. Elevated expression of neuropilin-2 associated with unfavorable prognosis in hepatocellular carcinoma. Onco Targets Ther. 2017 Jul 31;10:3827–33.

99. Bergé M, Allanic D, Bonnin P, De Montrion C, Richard J, Suc M, Boivin JF, Contrers JO, Lockhart BP, Pocard M, Lévy BI, Tucker GC, Tobelem G, Merkulova-Rainon T. Neuropilin-1 is upregulated in hepatocellular carcinoma and contributes to tumour growth and vascular remodelling. J Hepatol. 2011 Oct 1;55(4):866–75.

100. Grandclement C, Borg C. Neuropilins: A new target for cancer therapy. Vol. 3, Cancers. 2011. p. 1899–928.

101. Prud'homme GJ, Glinka Y. Neuropilins are multifunctional coreceptors involved in tumor initiation, growth, metastasis and immunity. Oncotarget. 2012 Sep;3(9):921–39.

102. Chen L, Miao W, Tang X, Zhang H, Wang S, Luo F, Yan J. Inhibitory effect of neuropilin-1 monoclonal antibody (NRP-1 MAb) on glioma tumor in mice. J Biomed Nanotechnol. 2013;9(4):551–8.

103. Caunt M, Mak J, Liang W-C, Stawicki S, Pan Q, Tong RK, Kowalski J, Ho C, Reslan HB, Ross J, Berry L, Kasman I, Zlot C, Cheng Z, Le Couter J, Filvaroff EH, Plowman G, Peale F, French D, Carano R, Koch AW, Wu Y, Watts RJ, Tessier-Lavigne M, Bagri A. Blocking Neuropilin-2 Function Inhibits Tumor Cell Metastasis. Cancer Cell. 2008;13(4):331–42.

104. De Vlaeminck Y, Bonelli S, Awad RM, Dewilde M, Rizzolio S, Lecocq Q, Bolli E, Santos AR, Laoui D, Schoonooghe S. Targeting Neuropilin-1 with Nanobodies Reduces Colorectal Carcinoma Development. Cancers (Basel). 2020;12(12):3582.

105. Song H, Zhang J, Wang W, Huang P, Zhang Y, Liu J, Li C, Kong D. Acid-responsive PEGylated doxorubicin prodrug nanoparticles for neuropilin-1 receptor-mediated targeted drug delivery. Colloids Surfaces B Biointerfaces. 2015;136:365–74.

106. Kumar A, Huo S, Zhang X, Liu J, Tan A, Li S, Jin S, Xue X, Zhao Y, Ji T. Neuropilin-1-targeted gold nanoparticles enhance therapeutic efficacy of platinum (IV) drug for prostate cancer treatment. ACS Nano. 2014;8(5):4205–20.

107. Pushpakom S, Iorio F, Eyers PA, Escott KJ, Hopper S, Wells A, Doig A, Guilliams T, Latimer J, McNamee C, Norris A, Sanseau P, Cavalla D, Pirmohamed M. Drug repurposing: Progress, challenges and recommendations. Vol. 18, Nature Reviews Drug Discovery. 2018. p. 41–58.

108. Antoszczak M, Markowska A, Markowska J, Huczyński A. Old wine in new bottles: Drug

repurposing in oncology. Eur J Pharmacol. 2020;866:172784.

109. Hu T, Li P, Luo Z, Chen X, Zhang J, Wang C, Chen P, Dong Z. Chloroquine inhibits hepatocellular carcinoma cell growth in vitro and in vivo. Oncol Rep. 2016;35(1):43–9.

110. Elliott IA, Dann AM, Xu S, Kim SS, Abt ER, Kim W, Poddar S, Moore A, Zhou L, Williams JL, Capri JR, Ghukasyan R, Matsumura C, Tucker DA, Armstrong WR, Cabebe AE, Wu N, Li L, Le TM, Radu CG, Donahue TR. Lysosome inhibition sensitizes pancreatic cancer to replication stress by aspartate depletion. Proc Natl Acad Sci. 2019 Apr 2;116(14):6842 LP – 6847.

111. Zheng Y, Zhao YL, Deng X, Yang S, Mao Y, Li Z, Jiang P, Zhao X, Wei Y. Chloroquine inhibits colon cancer cell growth in vitro and tumor growth in vivo via induction of apoptosis. Cancer Invest. 2009;27(3):286–92.

112. Kim EL, Wüstenberg R, Rübsam A, Schmitz-Salue C, Warnecke G, Bücker EM, Pettkus N, Speidel D, Rohde V, Schulz-Schaeffer W, Deppert W, Giese A. Chloroquine activates the p53 pathway and induces apoptosis in human glioma cells. Neuro Oncol. 2010;12(4):389–400.

113. Sotelo J, Briceño E, López-González MA. Adding chloroquine to conventional treatment for glioblastoma multiforme: A randomized, double-blind, placebo-controlled trial. Ann Intern Med. 2006;144(5):337–43.

114. Xu R, Ji Z, Xu C, Zhu J. The clinical value of using chloroquine or hydroxychloroquine as autophagy inhibitors in the treatment of cancers A systematic review and meta-analysis. Vol. 97, Medicine (United States). 2018.

115. Sasaki K, Tsuno NH, Sunami E, Tsurita G, Kawai K, Okaji Y, Nishikawa T, Shuno Y, Hongo K, Hiyoshi M, Kaneko M, Kitayama J, Takahashi K, Nagawa H. Chloroquine potentiates the anti-cancer effect of 5-fluorouracil on colon cancer cells. BMC Cancer. 2010;10.

116. Marina N. LONG-TERM SURVIVORS OF CHILDHOOD CANCER: The Medical Consequences of Cure. Pediatr Clin North Am. 1997;44(4):1021–42.

117. Thorn CF, Oshiro C, Marsh S, Hernandez-Boussard T, McLeod H, Klein TE, Altman RB. Doxorubicin pathways: Pharmacodynamics and adverse effects. Pharmacogenet Genomics. 2011;21(7):440–6.

118. Astolfi L, Ghiselli S, Guaran V, Chicca M, Simoni E, Olivetto E, Lelli G, Martini A. Correlation of adverse effects of cisplatin administration in patients affected by solid tumours: A retrospective evaluation. Oncol Rep. 2013;29(4):1285–92.

119. Lee YT, Tan YJ, Oon CE. Molecular targeted therapy: Treating cancer with specificity. Vol. 834, European Journal of Pharmacology. 2018. p. 188–96.

120. Shuptrine CW, Surana R, Weiner LM. Monoclonal antibodies for the treatment of cancer. Vol. 22, Seminars in Cancer Biology. 2012. p. 3–13.

121. Yun WJ, Shin E, Lee K, Jung HY, Kim SH, Park Y-N, Yu E, Jang J-J. Clinicopathologic implication of hepatic progenitor cell marker expression in hepatoblastoma. Pathol - Res Pract. 2013;209(9):568–73.

122. Armeanu-Ebinger S, Hoh A, Wenz J, Fuchs J. Targeting EpCAM (CD326) for immunotherapy in hepatoblastoma. Oncoimmunology. 2013;2(1).

123. Turner NC, Ro J, André F, Loi S, Verma S, Iwata H, Harbeck N, Loibl S, Huang Bartlett C, Zhang K, Giorgetti C, Randolph S, Koehler M, Cristofanilli M. Palbociclib in Hormone-

Receptor–Positive Advanced Breast Cancer. N Engl J Med. 2015 Jun 1;373(3):209–19.

124. Xin M, Li R, Xie M, Park D, Owonikoko TK, Sica GL, Corsino PE, Zhou J, Ding C, White MA, Magis AT, Ramalingam SS, Curran WJ, Khuri FR, Deng X. Small-molecule Bax agonists for cancer therapy. Nat Commun. 2014;5.

125. Kim G, Ison G, McKee AE, Zhang H, Tang S, Gwise T, Sridhara R, Lee E, Tzou A, Philip R, Chiu HJ, Ricks TK, Palmby T, Russell AM, Ladouceur G, Pfuma E, Li H, Zhao L, Liu Q, Venugopal R, Ibrahim A, Pazdur R. FDA approval summary: Olaparib monotherapy in patients with deleterious germline BRCA-mutated advanced ovarian cancer treated with three or more lines of chemotherapy. Clin Cancer Res. 2015;21(19):4257–61.

126. Kats D, Ricker CA, Berlow NE, Noblet B, Nicolle D, Mevel K, Branchereau S, Judde JG, Stiverson CD, Stiverson CL, Svalina MN, Settelmeyer T, Matlock K, Lathara M, Mussini C, Geller JI, Noakes C, Sloma I, Bharathy N, Cairo S, Keller C. Volasertib preclinical activity in high-risk hepatoblastoma. Oncotarget. 2019;10(60):6403–17.

127. Hooks KB, Audoux J, Fazli H, Lesjean S, Ernault T, Dugot-Senant N, Leste-Lasserre T, Hagedorn M, Rousseau B, Danet C, Branchereau S, Brugières L, Taque S, Guettier C, Fabre M, Rullier A, Buendia M-A, Commes T, Grosset CF, Raymond A-A. New insights into diagnosis and therapeutic options for proliferative hepatoblastoma. Hepatology. 2018 Jul 1;68(1):89–102.

128. Shanmugam N, Valamparampil JJ, Scott JX, Vij M, Narasimhan G, Reddy MS, Rela M. Complete remission of refractory hepatoblastoma after liver transplantation in a child with sorafenib monotherapy: A new hope? Pediatr Blood Cancer. 2017 Dec 1;64(12):e26701.

129. Bulaklak K, Gersbach CA. The once and future gene therapy. Nat Commun. 2020;11(1):5820.

130. Rupaimoole R, Slack FJ. MicroRNA therapeutics: towards a new era for the management of cancer and other diseases. Nat Rev Drug Discov. 2017;16(3):203–22.

131. Stadtmauer EA, Fraietta JA, Davis MM, Cohen AD, Weber KL, Lancaster E, Mangan PA, Kulikovskaya I, Gupta M, Chen F, Tian L, Gonzalez VE, Xu J, Jung I young, Joseph Melenhorst J, Plesa G, Shea J, Matlawski T, Cervini A, Gaymon AL, Desjardins S, Lamontagne A, Salas-Mckee J, Fesnak A, Siegel DL, Levine BL, Jadlowsky JK, Young RM, Chew A, Hwang WT, Hexner EO, Carreno BM, Nobles CL, Bushman FD, Parker KR, Qi Y, Satpathy AT, Chang HY, Zhao Y, Lacey SF, June CH. CRISPR-engineered T cells in patients with refractory cancer. Science (80- ). 2020;367(6481).

132. Lu Y, Xue J, Deng T, Zhou X, Yu K, Deng L, Huang M, Yi X, Liang M, Wang Y, Shen H, Tong R, Wang W, Li L, Song J, Li J, Su X, Ding Z, Gong Y, Zhu J, Wang Y, Zou B, Zhang Y, Li Y, Zhou L, Liu Y, Yu M, Wang Y, Zhang X, Yin L, Xia X, Zeng Y, Zhou Q, Ying B, Chen C, Wei Y, Li W, Mok T. Safety and feasibility of CRISPR-edited T cells in patients with refractory non-small-cell lung cancer. Nat Med. 2020;26(5):732–40.

133. Indersie E, Lesjean S, Hooks KB, Sagliocco F, Ernault T, Cairo S, Merched-Sauvage M, Rullier A, Le Bail B, Taque S, Grotzer M, Branchereau S, Guettier C, Fabre M, Brugières L, Hagedorn M, Buendia M-A, Grosset CF. MicroRNA therapy inhibits hepatoblastoma growth in vivo by targeting β-catenin and Wnt signaling . Hepatol Commun. 2017;1(2):168–83.

134. Cartier F, Indersie E, Lesjean S, Charpentier J, Hooks KB, Ghousein A, Desplat A, Dugot-Senant N, Trézéguet V, Sagliocco F, Hagedorn M, Grosset CF. New tumor suppressor microRNAs target glypican-3 in human liver cancer. Oncotarget. 2017;8(25):41211–26.

135. Schlom J, Vergati M, Intrivici C, Huen NY, Tsang KY. Strategies for cancer vaccine

development. Vol. 2010, Journal of Biomedicine and Biotechnology. 2010.

136. Doi I. Establishment of a cell line and its clonal sublines from a patient with hepatoblastoma. Gann, Japanese J Cancer Res. 1976;67(1):1–10.

137. López-Terrada D, Cheung SW, Finegold MJ, Knowles BB. Hep G2 is a hepatoblastoma-derived cell line. Vol. 40, Human Pathology. 2009. p. 1512–5.

138. Eloranta K, Cairo S, Liljeström E, Soini T, Kyrönlahti A, Judde JG, Wilson DB, Heikinheimo M, Pihlajoki M. Chloroquine Triggers Cell Death and Inhibits PARPs in Cell Models of Aggressive Hepatoblastoma. Front Oncol. 2020;10.

139. Arceci RJ, King AA, Simon MC, Orkin SH, Wilson DB. Mouse GATA-4: a retinoic acid-inducible GATA-binding transcription factor expressed in endodermally derived tissues and heart. Mol Cell Biol. 1993;13(4):2235–46.

140. Dunning MJ, Smith ML, Ritchie ME, Tavaré S. Beadarray: R classes and methods for Illumina bead-based data. Bioinformatics. 2007;23(16):2183–4.

141. Smyth GK. Linear models and empirical bayes methods for assessing differential expression in microarray experiments. Stat Appl Genet Mol Biol. 2004;3(1).

142. Barrett T, Wilhite SE, Ledoux P, Evangelista C, Kim IF, Tomashevsky M, Marshall KA, Phillippy KH, Sherman PM, Holko M. NCBI GEO: archive for functional genomics data sets—update. Nucleic Acids Res. 2012;41(D1):D991–5.

143. Bolger AM, Lohse M, Usadel B. Trimmomatic: A flexible trimmer for Illumina sequence data. Bioinformatics. 2014;30(15):2114–20.

144. Kim D, Langmead B, Salzberg SL. HISAT: A fast spliced aligner with low memory requirements. Nat Methods. 2015;12(4):357–60.

145. Robinson MD, McCarthy DJ, Smyth GK. edgeR: A Bioconductor package for differential expression analysis of digital gene expression data. Bioinformatics. 2009;26(1):139–40.

146. Gürtler A, Kunz N, Gomolka M, Hornhardt S, Friedl AA, McDonald K, Kohn JE, Posch A. Stain-Free technology as a normalization tool in Western blot analysis. Anal Biochem. 2013;433(2):105–11.

147. Guzmán C, Bagga M, Kaur A, Westermarck J, Abankwa D. ColonyArea: An ImageJ plugin to automatically quantify colony formation in clonogenic assays. PLoS One. 2014;9(3).

148. Schneider CA, Rasband WS, Eliceiri KW. NIH Image to ImageJ: 25 years of image analysis. Vol. 9, Nature Methods. 2012. p. 671–5.

149. Chong J, Wishart DS, Xia J. Using MetaboAnalyst 4.0 for Comprehensive and Integrative Metabolomics Data Analysis. Curr Protoc Bioinforma. 2019;68(1).

150. Ren JG, Seth P, Everett P, Clish CB, Sukhatme VP. Induction of erythroid differentiation in human erythroleukemia cells by depletion of malic enzyme 2. PLoS One. 2010;5(9):1–12.

151. Chen W, Kozielski R, LeVea C, Chen F. The Advances in Molecular Biology of Hepatoblastoma: Implications for Diagnostic Pathology. Am Chinese J Med Sci. 2012;5(4):217.

152. Zhou Y, Chang H, Yang B. Gata4 is upregulated in nasopharyngeal cancer and facilitates epithelial-mesenchymal transition and metastasis through regulation of slug. Exp Ther Med. 2018;16(6):5318–26.

153. Kyrönlahti A, Kauppinen M, Lind E, Unkila-Kallio L, Butzow R, Klefström J, Wilson DB, Anttonen M, Heikinheimo M. GATA4 protects granulosa cell tumors from TRAIL-induced apoptosis. Endocr Relat Cancer. 2010;17(3):709–17.

154. Han Q, Xu X, Li J, Wang J, Bai L, Wang A, Wang W, Zhang B. GATA4 is highly expressed in childhood acute lymphoblastic leukemia, promotes cell proliferation and inhibits apoptosis by activating BCL2 and MDM2. Mol Med Rep. 2017;16(5):6290–8.

155. Soini T, Haveri H, Elo JM, Kauppinen M, Kyrönlahti A, Salo MK, Lohi J, Andersson LC, Wilson DB, Heikinheimo M. Transcription factor GATA-4 is abundantly expressed in childhood but not in adult liver tumors. J Pediatr Gastroenterol Nutr. 2012;

156. Dame C, Sola MC, Lim KC, Leach KM, Fandrey J, Ma Y, Knöpfle G, Engel JD, Bungert J. Hepatic Erythropoietin Gene Regulation by GATA-4. J Biol Chem. 2004;279(4):2955–61.

157. Soini T, Pihlajoki M, Kyrönlahti A, Andersson LC, Wilson DB, Heikinheimo M. Downregulation of transcription factor GATA4 sensitizes human hepatoblastoma cells to doxorubicin-induced apoptosis. Tumor Biol. 2017;39(3).

158. Pei Y, Yao Q, Yuan S, Xie B, Liu Y, Ye C, Zhuo H. GATA4 promotes hepatoblastoma cell proliferation by altering expression of miR125b and DKK3. Oncotarget. 2016 Nov 22;7(47):77890–901.

159. Holtzinger A, Evans T. Gata4 regulates the formation of multiple organs. Development. 2005;132(17):4005–14.

160. Ashburner M, Ball CA, Blake JA, Botstein D, Butler H, Cherry JM, Davis AP, Dolinski K, Dwight SS, Eppig JT, Harris MA, Hill DP, Issel-Tarver L, Kasarskis A, Lewis S, Matese JC, Richardson JE, Ringwald M, Rubin GM, Sherlock G. Gene ontology: Tool for the unification of biology. Vol. 25, Nature Genetics. 2000. p. 25–9.

161. Thiery JP, Acloque H, Huang RYJ, Nieto MA. Epithelial-Mesenchymal Transitions in Development and Disease. Vol. 139, Cell. 2009. p. 871–90.

162. Lamouille S, Xu J, Derynck R. Molecular mechanisms of epithelial-mesenchymal transition. Vol. 15, Nature Reviews Molecular Cell Biology. 2014. p. 178–96.

163. Van Zijl F, Krupitza G, Mikulits W. Initial steps of metastasis: Cell invasion and endothelial transmigration. Vol. 728, Mutation Research - Reviews in Mutation Research. 2011. p. 23–34.

164. Cano A, Pérez-Moreno MA, Rodrigo I, Locascio A, Blanco MJ, Del Barrio MG, Portillo F, Nieto MA. The transcription factor Snail controls epithelial-mesenchymal transitions by repressing E-cadherin expression. Nat Cell Biol. 2000;2(2):76–83.

165. Cary LA, Chang JF, Guan JL. Stimulation of cell migration by overexpression of focal adhesion kinase and its association with Src and Fyn. J Cell Sci. 1996;109(7):1787–94.

166. Benbow U, Schoenermark MP, Mitchell TI, Rutter JL, Shimokawa K, Nagase H, Brinckerhoff CE. A Novel Host/Tumor Cell Interaction Activates Matrix Metalloproteinase 1 and Mediates Invasion through Type I Collagen*. J Biol Chem. 1999;274(36):25371–8.

167. Zheng R, Rebolledo-Jaramillo B, Zong Y, Wang L, Russo P, Hancock W, Stanger BZ, Hardison RC, Blobel GA. Function of GATA factors in the adult mouse liver. PLoS One. 2013;

168. Tamaru S, Fukuta T, Kaibuchi K, Matsuoka Y, Shiku H, Nishikawa M. Rho-kinase induces association of adducin with the cytoskeleton in platelet activation. Biochem Biophys Res Commun. 2005;332(2):347–51.

169. Sudo H, Tsuji AB, Sugyo A, Abe M, Hino O, Saga T. AHNAK is highly expressed and plays a key role in cell migration and invasion in mesothelioma. Int J Oncol. 2014;44(2):530–8.

170. Campbell K, Whissell G, Franch-Marro X, Batlle E, Casanova J. Specific GATA Factors Act as Conserved Inducers of an Endodermal-EMT. Dev Cell. 2011;21(6):1051–61.

171. Hazan RB, Kang L, Whooley BP, Borgen PI. N-Cadherin Promotes Adhesion between Invasive Breast Cancer Cells and the Stroma. Cell Commun Adhes. 1997;4(6):399–411.

172. Song W, Jackson K, McGuire PG. Degradation of type IV collagen by matrix metalloproteinases is an important step in the epithelial-mesenchymal transformation of the endocardial cushions. Dev Biol. 2000;

173. Wang SJ, Cui HY, Liu YM, Zhao P, Zhang Y, Fu ZG, Chen ZN, Jiang JL. CD147 promotes Src-dependent activation of Rac1 signaling through STAT3/DOCK8 during the motility of hepatocellular carcinoma cells. Oncotarget. 2015;6(1):243–57.

174. IRWIN J. Insulin-like growth factor binding protein-1 (IGFBP-1) modulates placental cytotrophoblast interaction with fibronectin In vitro. J Soc Gynecol Investig. 1995;2(2):360.

175. Schor SL, Schor AM, Grey AM, Rushton G. Foetal and cancer patient fibroblasts produce an autocrine migration-stimulating factor not made by normal adult cells. J Cell Sci. 1988;90(3):391–9.

176. Bousquet E, Mazières J, Privat M, Rizzati V, Casanova A, Ledoux A, Mery E, Couderc B, Favre G, Pradines A. Loss of RhoB expression promotes migration and invasion of human bronchial cells via activation of AKT1. Cancer Res. 2009;69(15):6092–9.

177. Zhang JS, Koenig A, Young C, Billadeau DD. GRB2 couples RhoU to epidermal growth factor receptor signaling and cell migration. Mol Biol Cell. 2011;22(12):2119–30.

178. Sung HY, Han J, Ju W, Ahn JH. Synaptotagmin-like protein 2 gene promotes the metastatic potential in ovarian cancer. Oncol Rep. 2016;36(1):535–41.

179. Araki K, Shimura T, Suzuki H, Tsutsumi S, Wada W, Yajima T, Kobayahi T, Kubo N, Kuwano H. E/N-cadherin switch mediates cancer progression via TGF-β-induced epithelial-to-mesenchymal transition in extrahepatic cholangiocarcinoma. Br J Cancer. 2011;105(12):1885–93.

180. Zhitnyak IY, Rubtsova SN, Litovka NI, Gloushankova NA. Early Events in Actin Cytoskeleton Dynamics and E-Cadherin-Mediated Cell-Cell Adhesion during Epithelial-Mesenchymal Transition. Cells. 2020;9(3):578.

181. Jaksik R, Iwanaszko M, Rzeszowska-Wolny J, Kimmel M. Microarray experiments and factors which affect their reliability. Biol Direct. 2015 Sep 3;10:46.

182. Enane FO, Shuen WH, Gu X, Quteba E, Przychodzen B, Makishima H, Bodo J, Ng J, Chee CL, Ba R, Koh LS, Lim J, Cheong R, Teo M, Hu Z, Ng KP, Maciejewski J, Radivoyevitch T, Chung A, Ooi LL, Tan YM, Cheow PC, Chow P, Chan CY, Lim KH, Yerian L, Hsi E, Toh HC, Saunthararajah Y. GATA4 loss of function in liver cancer impedes precursor to hepatocyte transition. J Clin Invest. 2017;127(9):3527–42.

183. Pellet-Many C, Frankel P, Jia H, Zachary I. Neuropilins: Structure, function and role in disease. Vol. 411, Biochemical Journal. 2008. p. 211–26.

184. Nasarre P, Gemmill RM, Drabkin HA. The emerging role of class-3 semaphorins and their neuropilin receptors in oncology. Vol. 7, OncoTargets and Therapy. 2014. p. 1663–87.

185. Niland S, Eble JA. Neuropilin: Handyman and Power Broker in the Tumor Microenvironment. In: Advances in Experimental Medicine and Biology. 2020. p. 31–67.

186. Schulz A, Gorodetska I, Behrendt R, Fuessel S, Erdmann K, Foerster S, Datta K, Mayr T, Dubrovska A, Muders MH. Linking NRP2 With EMT and Chemoradioresistance in Bladder Cancer. Front Oncol. 2020;9:1461.

187. Tu DG, Chang WW, Jan MS, Tu CW, Lu YC, Tai CK. Promotion of metastasis of thyroid cancer cells via NRP-2-mediated induction. Oncol Lett. 2016;12(5):4224–30.

188. Lin J, Zhang Y, Wu J, Li L, Chen N, Ni P, Song L, Liu X. Neuropilin 1 (NRP1) is a novel tumor marker in hepatocellular carcinoma. Clin Chim Acta. 2018;485:158–65.

189. Wittmann P, Grubinger M, Gröger C, Huber H, Sieghart W, Peck-Radosavljevic M, Mikulits W. Neuropilin-2 induced by transforming growth factor-β augments migration of hepatocellular carcinoma cells. BMC Cancer. 2015 Nov 16;15:909.

190. Cong L, Ran FA, Cox D, Lin S, Barretto R, Habib N, Hsu PD, Wu X, Jiang W, Marraffini LA, Zhang F. Multiplex genome engineering using CRISPR/Cas systems. Science (80- ). 2013;339(6121):819–23.

191. Zhao M, Zhang M, Tao Z, Cao J, Wang L, Hu X. miR-331-3p Suppresses Cell Proliferation in TNBC Cells by Downregulating NRP2. Technol Cancer Res Treat. 2020;19.

192. Samuel S, Gaur P, Fan F, Xia L, Gray MJ, Dallas NA, Bose D, Rodriguez-Aguayo C, Lopez-Berestein G, Plowman G, Bagri A, Sood AK, Ellis LM. Neuropilin-2 mediated β-catenin signaling and survival in human gastro-intestinal cancer cell lines. PLoS One. 2011;6(10).

193. Fujii T, Shimada K, Asano A, Tatsumi Y, Yamaguchi N, Yamazaki M, Konishi N. MicroRNA-331-3p suppresses cervical cancer cell proliferation and E6/E7 expression by targeting NRP2. Int J Mol Sci. 2016;17(8).

194. Rodrigo M, Buchtelova H, Jimenez A, Adam P, Babula P, Heger Z, Adam V. Transcriptomic Landscape of Cisplatin-Resistant Neuroblastoma Cells. Vol. 8, Cells. 2019. p. 235.

195. Besharat ZM, Sabato C, Po A, Gianno F, Abballe L, Napolitano M, Miele E, Giangaspero F, Vacca A, Catanzaro G, Ferretti E. Low expression of miR-466f-3p sustains epithelial to mesenchymal transition in sonic hedgehog medulloblastoma stem cells through Vegfa-Nrp2 signaling pathway. Front Pharmacol. 2018;9(NOV).

196. Guillon MAM, Mary PMJ, Brugière L, Marec-Bérard P, Pacquement HD, Schmitt C, Guinebretière JM, Tabone MDP. Clinical characteristics and prognosis of osteosarcoma in young children: A retrospective series of 15 cases. BMC Cancer. 2011;11.

197. Yilmaz M, Christofori G. EMT, the cytoskeleton, and cancer cell invasion. Vol. 28, Cancer and Metastasis Reviews. 2009. p. 15–33.

198. Yasuoka H, Kodama R, Tsujimoto M, Yoshidome K, Akamatsu H, Nakahara M, Inagaki M, Sanke T, Nakamura Y. Neuropilin-2 expression in breast cancer: correlation with lymph node metastasis, poor prognosis, and regulation of CXCR4 expression. BMC Cancer. 2009;9:220.

199. Gomes LR, Menck CFM, Leandro GS. Autophagy roles in the modulation of DNA repair pathways. Vol. 18, International Journal of Molecular Sciences. 2017.

200. Parkhitko AA, Priolo C, Coloff JL, Yun J, Wu JJ, Mizumura K, Xu W, Malinowska IA, Yu

J, Kwiatkowski DJ, Locasale JW, Asara JM, Choi AMK, Finkel T, Henske EP. Autophagy-dependent metabolic reprogramming sensitizes tsc2-deficient cells to the antimetabolite 6-aminonicotinamide. Mol Cancer Res. 2014;12(1):48–57.

201. Chang Y, Chen L, Liu Y, Hu L, Li L, Tu Q, Wang R, Wu M, Yang J, Wang H. Inhibition of autophagy may suppress the development of hepatoblastoma. FEBS J. 2011;

202. Jiang P-D, Zhao Y-L, Shi W, Deng X-Q, Xie G, Mao Y-Q, Li Z-G, Zheng Y-Z, Yang S-Y, Wei Y-Q. Cell Growth Inhibition, $G_2$/M Cell Cycle Arrest, and Apoptosis Induced by Chloroquine in Human Breast Cancer Cell Line Bcap-37. Cell Physiol Biochem. 2008;22(5–6):431–40.

203. Lozy F, Karantza V. Autophagy and cancer cell metabolism. Vol. 23, Seminars in Cell and Developmental Biology. 2012. p. 395–401.

204. Cantó C, Menzies KJ, Auwerx J. NAD+ Metabolism and the Control of Energy Homeostasis: A Balancing Act between Mitochondria and the Nucleus. Cell Metabolism. 2015.

205. Schuster S, Penke M, Gorski T, Gebhardt R, Weiss TS, Kiess W, Garten A. FK866-induced NAMPT inhibition activates AMPK and downregulates mTOR signaling in hepatocarcinoma cells. Biochem Biophys Res Commun. 2015;458(2):334–40.

206. Ju H-Q, Zhuang Z-N, Li H, Tian T, Lu Y-X, Fan X-Q, Zhou H-J, Mo H-Y, Sheng H, Chiao PJ, Xu R-H. Regulation of the Nampt-mediated NAD salvage pathway and its therapeutic implications in pancreatic cancer. Cancer Lett. 2016;379(1):1–11.

207. Yelamos J, Farres J, Llacuna L, Ampurdanes C, Martin-Caballero J. PARP-1 and PARP-2: New players in tumour development. Am J Cancer Res. 2011;1(3):328–46.

208. Gibson BA, Kraus WL. New insights into the molecular and cellular functions of poly(ADP-ribose) and PARPs. Vol. 13, Nature Reviews Molecular Cell Biology. 2012. p. 411–24.

209. Gelmon KA, Tischkowitz M, Mackay H, Swenerton K, Robidoux A, Tonkin K, Hirte H, Huntsman D, Clemons M, Gilks B, Yerushalmi R, Macpherson E, Carmichael J, Oza A. Olaparib in patients with recurrent high-grade serous or poorly differentiated ovarian carcinoma or triple-negative breast cancer: A phase 2, multicentre, open-label, non-randomised study. Lancet Oncol. 2011;12(9):852–61.

210. Robson M, Im S-A, Senkus E, Xu B, Domchek SM, Masuda N, Delaloge S, Li W, Tung N, Armstrong A, Wu W, Goessl C, Runswick S, Conte P. Olaparib for Metastatic Breast Cancer in Patients with a Germline BRCA Mutation . N Engl J Med. 2017;377(6):523–33.

211. Valanejad L, Cast A, Wright M, Bissig KD, Karns R, Weirauch MT, Timchenko N. PARP1 activation increases expression of modified tumor suppressors and pathways underlying development of aggressive hepatoblastoma. Commun Biol. 2018;1(1).

212. Zai W, Chen W, Han Y, Wu Z, Fan J, Zhang X, Luan J, Tang S, Jin X, Fu X, Gao H, Ju D, Liu H. Targeting PARP and autophagy evoked synergistic lethality in hepatocellular carcinoma. Carcinogenesis. 2020;41(3):345–57.

213. Rizzolio S, Tamagnone L. Multifaceted Role of Neuropilins in Cancer. Curr Med Chem. 2011;18(23):3563–75.

214. Verbaanderd C, Maes H, Schaaf MB, Sukhatme VP, Pantziarka P, Sukhatme V, Agostinis P, Bouche G. Repurposing drugs in oncology (ReDO) - Chloroquine and hydroxychloroquine as anti-cancer agents. Ecancermedicalscience. 2017;11.